

1 Title

2 Large-scale clustering of longitudinal faecal calprotectin and C-reactive protein
3 profiles in inflammatory bowel disease

4 Short title

5 Longitudinal biomarker clustering in inflammatory bowel disease

6 Authors

7 Nathan Constantine-Cooke^{1,2}, Nikolas Plevris^{1,3}, Karla Monterrubio-Gómez^{1,2}, Clara
8 Ramos Belinchón^{1,3}, Solomon Ong³, Alexander T. Elford^{3,4}, Beatriz Gros^{3,5}, Gareth-
9 Rhys Jones^{3,6}, Charlie W. Lees^{† 1,3} and Catalina A. Vallejos^{† 2}.

10 † Joint senior authors

11 Affiliations

- 12 1. Centre for Genomic and Experimental Medicine, Institute of Genetics and
13 Cancer, University of Edinburgh, Edinburgh, UK
- 14 2. MRC Human Genetics Unit, Institute of Genetics and Cancer, University of
15 Edinburgh, Edinburgh, UK
- 16 3. Edinburgh IBD Unit, Western General Hospital, Edinburgh, UK
- 17 4. Faculty of Medicine, The University of Melbourne, Melbourne, Australia
- 18 5. Reina Sofía University Hospital, Gastroenterology and Hepatology. IMIBIC.
19 University of Cordoba. Cordoba, Spain
- 20 6. Centre for Inflammation Research, The Queen's Medical Research Institute,
21 University of Edinburgh, Edinburgh, UK

22 Abstract

23 Background

24 Crohn's disease (CD) and ulcerative colitis (UC) are highly heterogeneous, dynamic
25 and unpredictable, with a marked disconnect between symptoms and intestinal

NOTE: This preprint reports new research that has not been certified by peer review and should not be used to guide clinical practice.

26 inflammation. Attempts to classify inflammatory bowel disease (IBD) subphenotypes
27 to inform clinical decision making have been limited. We aimed to describe the latent
28 disease heterogeneity by modelling routinely collected faecal calprotectin (FC) and
29 CRP data, describing dynamic longitudinal inflammatory patterns in IBD.

30 Methods

31 In this retrospective study, we analysed patient-level longitudinal measurements of FC
32 and CRP recorded within seven years since diagnosis. Latent class mixed models
33 (LCMMs) were used to cluster individuals with similar longitudinal FC or CRP profiles.
34 Associations between cluster assignment and information available at diagnosis (e.g.
35 age, sex, and Montreal classification) were quantified using multinomial logistic
36 regression. Differences in advanced therapy use across clusters were also explored
37 using cumulative distributions over time. Finally, we considered uncertainty in cluster
38 assignments with respect to follow-up length and explored the overlap between
39 clusters identified based on FC and CRP.

40 Findings

41 We included 1036 patients (544 CD, 380 UC, 112 IBD-unclassified (IBDU)) in the FC
42 analysis with a total of 10545 FC observations (median 9 per subject, IQR 6–13). The
43 CRP analysis consisted of 1838 patients (805 CD, 847 UC, 186 IBDU) with 49364
44 CRP measurements (median 20 per subject; IQR 10–36). Eight distinct clusters of
45 inflammatory behaviour over time were identified by LCMM in each analysis. The
46 clusters, FC1-8 and CRP1-8, were ordered from the lowest cumulative inflammatory
47 burden to the highest. The clusters included groups with high diagnostic levels of
48 inflammation which rapidly normalised, groups where high inflammation levels
49 persisted throughout the full seven years of observation, and a series of intermediates
50 including delayed remitters and relapsing remitters.

51 CD and UC patients were unevenly distributed across the clusters. In CD, whilst
52 patients with upper GI involvement (L4) were less likely to be in FC1 and FC2, there
53 was no impact on ileal versus colonic disease on cluster assignment. In UC, male sex
54 was associated with the poorest prognostic cluster (FC8). The use and timing of
55 advanced therapy was associated with cluster assignment, with the highest use of
56 early advanced therapy in FC1. Of note, FC8 and CRP8 captured consistently high

57 patterns of inflammation despite a high proportion of patients receiving advanced
58 therapy, particularly for CD individuals (56.8% and 33.3%, respectively). We observed
59 that uncertainty in cluster assignments was higher for individuals with short
60 longitudinal follow-up, particularly between clusters capturing similar earlier
61 inflammation patterns. There was broadly poor agreement between FC and CRP
62 clusters in keeping with the need to monitor both in clinical practice.

63 Interpretation

64 Distinct patterns of inflammatory behaviour over time are evident in patients with IBD.
65 Cluster assignment is associated with disease type and both the use and timing of
66 advanced therapy. These data pave the way for a deeper understanding of disease
67 heterogeneity in IBD and enhanced patient stratification in the clinic.

68

69 Introduction

70 Inflammatory bowel disease (IBD), an umbrella term for Crohn's disease (CD),
71 ulcerative colitis (UC) and inflammatory bowel disease unclassified (IBDU), has a
72 prevalence of almost 1% in the UK population.^{1,2} The condition is characterised by
73 chronic relapsing and remitting inflammation of the gastrointestinal (GI) tract that
74 confers a host of debilitating symptoms, negatively impacting quality of life.^{3,4} Studies
75 have clearly demonstrated that uncontrolled inflammation of the GI tract increases the
76 risk of disease progression and complications including the development of colorectal
77 cancer,⁵ stricturing/penetrating complications and surgery.^{6,7} However, IBD is highly
78 heterogeneous with respect to symptoms, inflammatory burden, treatment response,
79 and long-term outcomes.

80 Current IBD classification methods are mostly based on historic nomenclature which
81 utilise baseline phenotypic characteristics and do not take into account the dynamic
82 and unpredictable nature of the disease. Attempts at developing prediction tools to
83 identify high risk patients have been made but again these use static clinical
84 parameters, dismissing the changing nature of the disease.⁸ Furthermore, they do not
85 take into account the influence of other factors, such as advanced therapy timing, on
86 the disease course. In the wake of the increasing prevalence of IBD and associated
87 healthcare burden, new methods to characterise the dynamic disease course and help

88 identify at-risk individuals who require aggressive therapy with close monitoring versus
89 those that need less intense input are essential.

90 The original IBSEN studies provided the first data on the clinical course of patients
91 with UC and CD during the first 10-years of diagnosis.^{9,10} However, these data were
92 based on predefined disease patterns, rather than data driven, utilising symptoms
93 alone. It is now widely accepted that there is a clear disconnect between inflammation
94 and symptoms in IBD,¹¹ therefore it is imperative characterisations of disease course
95 include objective parameters of inflammation.

96 C-reactive protein (CRP) and faecal calprotectin (FC) are well established tools for
97 monitoring patients with IBD, but are typically interpreted in terms of the most recent
98 measurement or short-term trends. Interrogation of long-term trends of inflammation
99 could greatly assist clinical decision making and improve prediction of future events.
100 Moreover, modelling inflammatory behaviour over time might be a key tool for
101 characterising the largely unexplained heterogeneity seen in IBD, and provide new
102 tools for disease sub-phenotyping beyond the current Montreal classification.¹²

103 In this study, we aimed to 1) identify groups of IBD patients with similar longitudinal
104 patterns of inflammation 2) determine if these groupings were associated with age,
105 sex, IBD type, Montreal classification, or early advanced therapy, and 3) explore
106 whether subjects with similar longitudinal FC profiles also share similar CRP profiles.

107 **Methods**

108 **Ethics**

109 This project was approved by the local Caldicott Guardian (Project ID: CRD18002,
110 registered NHS Lothian information asset #IAR-954). Patients or the public were not
111 involved in the design, conduct, reporting or dissemination plans of our research.

112 **Study design**

113 This was a retrospective cohort study. Patients with a confirmed diagnosis of IBD (as
114 per Lennard-Jones criteria)¹³ were followed up for a period of seven years from the
115 date of diagnosis. Baseline phenotype data (sex, age at diagnosis, IBD type, date of
116 diagnosis) were obtained from the Lothian IBD registry (LIBDR), a retrospective cohort

117 of patients receiving IBD care in Lothian, Scotland. The LIBDR is estimated to have
118 identified 94.3% of all true IBD patients in the area using a capture-recapture
119 approach.¹ Using a population level cohort reduces potential biases associated with
120 cohort recruitment.¹⁴ When available, additional phenotyping information was
121 extracted by the clinical team from electronic health records (TrakCare; InterSystems,
122 Cambridge, MA). This includes smoking and Montreal classification for disease
123 location, behaviour and extent, all recorded as per patient status at the time of
124 diagnosis. Data on prescribing of all advanced therapies, including start/stop dates,
125 were extracted from both TrakCare and NHS Lothian pharmacy databases. Primary
126 care prescribing data were not available. See Supplementary Note 1 for more detailed
127 definitions.

128 Inclusion/exclusion criteria

129 Subjects were required to have a confirmed diagnosis of IBD at any age and receive
130 secondary care for their condition from the NHS Lothian health board. Only subjects
131 with a recorded date of IBD diagnosis between 2005 and 2019 were included. The
132 lower bound for this criteria was established as FC testing was not routinely performed
133 prior to this date. The upper bound ensured subjects had the possibility of having at
134 least five years of follow-up at the time of data extraction.

135 For subjects which met the above requirements, the following criteria was applied to
136 their FC and/or CRP longitudinal measurements. Subjects were required to have a
137 diagnostic measurement (\pm three months of diagnosis, Figures [S1](#) and [S2](#)) and have
138 a further two observations available within seven years of diagnosis. If any biomarker
139 measurements were observed within three months prior to the recorded diagnosis
140 date, measurement time scales were realigned with respect to diagnosis ([Figure S3](#)).
141 Only non-censored observations were considered in this calculation for FC. For CRP,
142 this filtering was applied after preprocessing (see “Longitudinal measurements and
143 preprocessing” section), and subjects with constant biomarker measurements over
144 time were excluded. As the clustering analyses were performed separately for FC and
145 CRP, subjects did not need to meet the criteria for both biomarkers.

146 Statistical analysis

147 Cohort description

148 Continuous variables were summarised as their median and interquartile range (IQR).

149 Categorical variables were summarised as counts and percentages.

150 Longitudinal measurements and preprocessing

151 FC and CRP measurements were obtained from an extract by the local biochemistry
152 team describing tests recorded up to August 13, 2024. For each individual, all
153 measurements made within seven years from diagnosis were considered. Failed tests,
154 for example due to contamination, were discarded. All FC tests were performed from
155 stool samples using the same ELISA technology.¹⁵ Due to limits of detection,
156 observations $< 20 \mu\text{g/g}$ were recorded to $20 \mu\text{g/g}$ whilst observations $> 1250 \mu\text{g/g}$ were
157 mapped to $1250 \mu\text{g/g}$. Such observations were treated as censored when applying the
158 inclusion exclusion criteria described above. CRP was measured from blood samples;
159 observations for which only an upper bound was available, e.g. $< 1 \text{ mg/L}$, were
160 mapped to the corresponding upper bound.

161 Further processing was applied to CRP data to smooth out short-term fluctuations.
162 Measurements were grouped into intervals of t : $[0, 0.5)$, $[0.5, 1.5)$, $[1.5, 2.5)$, $[2.5, 3.5)$,
163 $[3.5, 4.5)$, $[4.5, 5.5)$, $[5.5, 7]$, where $t = 0$ (years) is the time of diagnosis. The median
164 CRP for each interval was calculated for each subject and used as input for
165 subsequent analyses. The centre of each interval was used as the corresponding
166 observation time.

167 Longitudinal biomarker clustering

168 Prior to model fitting, FC and CRP observations were log-transformed. FC and CRP
169 trajectories were modelled separately using latent class mixed models (LCMMs),¹⁶ an
170 extension of linear mixed effects models that enables clustering of individuals that
171 share similar longitudinal biomarker trajectories. LCMM consists of two submodels:
172 one which captures the longitudinal behaviour of the biomarker, and one which
173 captures cluster assignment. Fixed effects for the longitudinal submodel were
174 specified using natural cubic splines with three interior knots placed at quantiles with
175 respect to observation times. An alternative specification was considered leading to

176 similar results. Only the intercept was treated as a random effect. The cluster
177 assignment submodel used IBD type (CD, UC, and IBDU) as a covariate. Formal
178 definitions of the LCMM models considered here and the associated hyper-parameter
179 choices are provided in Supplementary Note 2.

180 As the number of clusters is not known a priori, the optimal model was found using a
181 grid search approach. We considered models with 2–10 clusters for both FC and CRP.
182 The likelihood based statistics,¹⁷ Akaike information criterion (AIC) and Bayesian
183 information criterion (BIC), and visual inspection of cluster trajectories were used to
184 compare models with different specifications and determine the most appropriate
185 number of assumed clusters.

186 LCMM calculates, for each individual, the probability of being assigned to each cluster.
187 In subsequent analysis, each individual was assigned to the cluster with the highest
188 probability. The distribution of cluster assignment probabilities was used to assess
189 uncertainty in these allocations with respect to follow-up length. This was defined as
190 the time difference between diagnosis and the last available biomarker measurement
191 (FC or CRP, depending on the analysis). For each cluster, the average probability of
192 individual-specific probabilities of cluster assignment were reported.

193 To avoid displaying potentially identifiable individual-level data, exemplar trajectories
194 within each cluster are visualised as aggregated trends, where measurements were
195 summarised as the median across six randomly selected individuals. Cluster labels
196 were ordered based on the area under the overall biomarker trend inferred for each
197 cluster (a proxy for cumulative inflammatory burden).

198 Associations with respect to cluster assignments

199 To facilitate the interpretation of each cluster, we considered potential associations
200 between cluster assignments and patient-level information. Violin plots and
201 percentage bar plots were used as a visual summary when considering continuous
202 (age) and discrete (sex, IBD type, additional phenotyping) patient-level covariates,
203 respectively. Associations with respect to additional phenotyping were only explored
204 after stratifying by IBD type (CD and UC only). Multinomial logistic regression was
205 used to quantify associations between cluster assignments and patient-level
206 covariates. The cluster used as the reference class was chosen to closely resemble
207 the overall distribution of IBD types within the corresponding cohort. Univariate and

208 multivariate models were considered, and the associated 95% confidence intervals
209 are reported. Individuals with missing covariate values were excluded when fitting
210 each model. Due to small cluster sizes and low frequency of some covariate levels,
211 the analysis was repeated after merging clusters with similar cumulative inflammatory
212 burden. Effect sizes were largely consistent (data not shown).

213 Advanced therapy use

214 To compare patterns of advanced therapy (AT) across clusters, the cumulative
215 distribution of first-line advanced therapy use was calculated. Results are reported
216 stratified by IBD type (CD and UC only).

217 Comparison between FC and CRP cluster assignments

218 For subjects meeting the criteria for both FC and CRP analyses, the relationship
219 between FC and CRP cluster assignment was visualised using alluvial plots and side-
220 by-side comparisons of mean cluster trajectories for the optimal models. Stratified
221 results for CD and UC subjects are also reported.

222 Software

223 R (v. 4.4.0), extended using the lcmm (v. 2.1.0),¹⁸ ggalluvial (v.0.12.5),¹⁹ and datefixR
224 (v.1.6.1)²⁰ packages, was used for all analyses. Analytical reports have been
225 generated using the Quarto scientific publishing system and are hosted online
226 (<https://vallejosgroup.github.io/Lothian-IBDR/>). An R package, libdr (v.1.0.0), has also
227 been produced, supporting the reuse of our R code with other datasets.

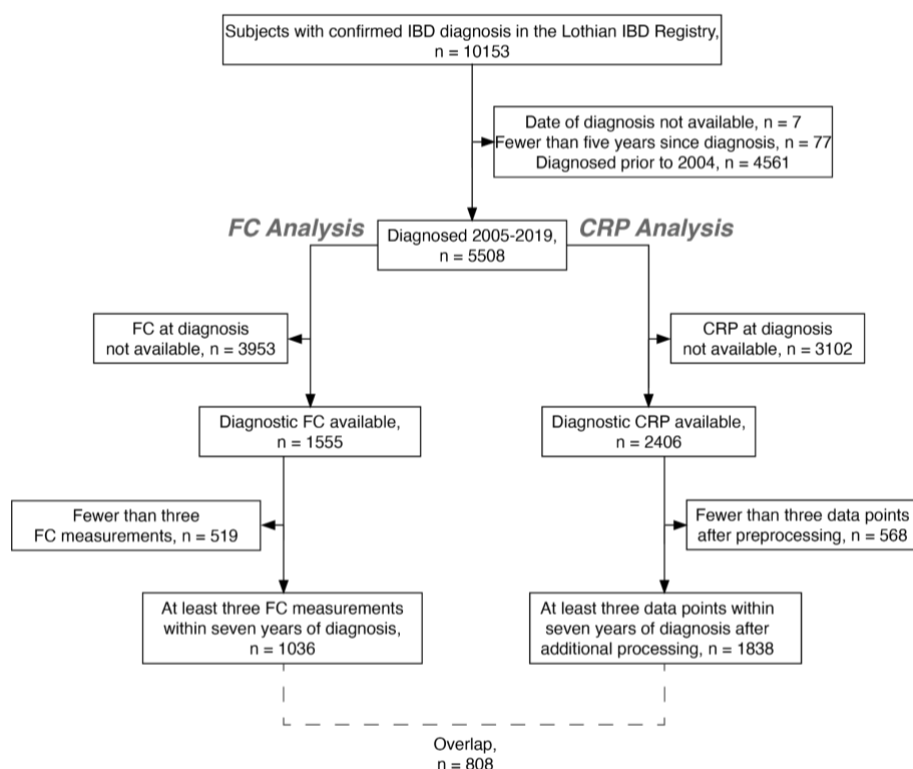
228 Role of the funding source

229 Funders were not involved in the study design, collection, analysis, or interpretation
230 of the data, writing, or decision to submit the paper for publication.

231 Results

232 Cohort derivation and description

233 Of the 10153 subjects with a confirmed IBD diagnosis, 5508 were reported as being
 234 diagnosed between 2005 and 2019 ([Figure 1](#)). Of these subjects, 1036 and 1838
 235 subjects were included in the FC and CRP analysis, respectively. We identified 808
 236 subjects which met the inclusion criteria for both biomarkers. [Table 1](#) describes key
 237 demographic factors for subjects included in the FC and CRP analyses.



238
 239 *Figure 1. Derivation of the study cohorts based on separate faecal calprotectin (FC) and C-reactive*
 240 *protein (CRP) inclusion/exclusion criteria.*

241

	FC analysis (n = 1036)	CRP analysis (n = 1838)	Overlap (n = 808)
Age at diagnosis	33 (25–75)	37 (24–55)	32 (20–50)
Male sex	503 (48.6%)	956 (52.0%)	397 (49.1%)
IBD type			
Crohn's disease (CD)	544 (52.5%)	805 (43.8%)	451 (55.8%)
Ulcerative colitis (UC)	380 (36.7%)	847 (46.1%)	276 (34.2%)

IBDU	112 (10.8%)	186 (10.1%)	81 (10.0%)
Baseline FC (µg/g)	740 (320–1070)	..	760 (330–1081)
FC observations	9 (6–13)	..	9 (6–14)
Baseline CRP (µg/mL)	..	8 (3–24)	8 (3–20)
Total unprocessed CRP observations	..	20 (10–36)	26 (14–36)
Total CRP observations after pre-processing	..	6 (4–7)	6 (5–7)
Advanced therapies (AT)			
AT within seven years for CD	270 (49.6%)	374 (46.5%)	
AT within one year for CD	129 (23.7%)	167 (20.7%)	
AT within seven years for UC	108 (28.4%)	85 (10.0%)	
AT within one year for UC	42 (11.1%)	35 (4.1%)	
Crohn's disease			
Montreal location			
L1	168 (30.9%)	249 (30.9%)	136 (30.2%)
L2	200 (36.8%)	287 (35.7%)	157 (34.8%)
L3	169 (31.1%)	246 (30.6%)	153 (33.9%)
Missing	7 (1.3%)	23 (2.9%)	5 (1.1%)
Upper GI inflammation			
Present	77 (14.2%)	87 (10.8%)	68 (15.1%)
Not Present	467 (85.8.4%)	718 (89.2%)	383 (84.9%)
Montreal behaviour			
B1	443 (81.4%)	607 (75.4%)	364 (80.7%)
B2	63 (11.5%)	110 (13.7%)	54 (12.0%)
B3	28 (5.1%)	61 (7.6%)	25 (5.5%)

Missing	10 (1.8%)	27 (3.4%)	8 (1.8%)
Perianal disease			
Present	79 (14.5%)	113 (14.0%)	68 (15.1%)
Not Present	459 (84.4%)	673 (83.6%)	379 (84.0%)
Missing	6 (1.1%)	19 (2.4%)	4 (0.9%)
Smoking status			
Current or previously	166 (30.5%)	274 (34.0%)	138 (30.6%)
Never	352 (64.7%)	484 (60.1%)	293 (65.0%)
Missing	26 (4.8%)	47 (5.8%)	20 (4.4%)

242 *Table 1. Demographic and clinical data at diagnosis for subjects meeting the faecal calprotectin (FC)*
 243 *or C-reactive protein (CRP) study inclusion criteria. Continuous data are presented as median and*
 244 *interquartile range. Categorical data are presented as counts and percentages. Missingness is only*
 245 *directly reported if values were missing. The column labelled as “Overlap” denotes subjects which met*
 246 *the inclusion criteria for both FC and CRP modelling. Missing observations for upper gastrointestinal*
 247 *inflammation were assumed to be “not present” (Supplementary Note 1). Missingness was not*
 248 *inferred to be a value for any other variable.*

249 Longitudinal measurements of FC and CRP

250 For subjects in the FC analysis, 10545 FC observations were available (median 9 per
 251 subject, IQR 6–13). Prior to processing 49364 CRP observations were available
 252 (median 20 per subject, IQR 10–36). Following the pre-processing of CRP
 253 observations, there were 9898 data points (median 6 per subject, IQR 4–7). The
 254 distribution of log-transformed FC and CRP values is shown in [Figure S4](#).

255 Modelling of FC trajectories

256 AIC suggested the 10-cluster model ([Figure S5](#)), whilst BIC suggested the 9-cluster
 257 model ([Figure S6](#)) was more appropriate ([Table S1](#), [Figure S7A](#)). However, the 8-
 258 cluster model was chosen as a parsimonious choice, as it captures the main observed
 259 longitudinal patterns without generating very small clusters (<50 individuals) which
 260 could be difficult to interpret.

261 [Figure 2](#) shows representative cluster profiles for the 8-cluster model, ordered from
 262 lowest (FC1) to highest (FC8) cumulative inflammatory burden. FC2 (n=67; ~6%)

263 represents low FC values throughout the whole observation period. Instead, FC1
264 (n=140; ~14%) and FC3 (n=157; ~15%) and FC7 (n=244; ~24%) were characterised
265 by initially high FC values (>250 µg/g) which decreased over time at different rates.
266 Whilst FC1 exhibited a sharp decrease within the first year, the decrease was more
267 gradual for FC3 and FC7, where FC was normalised (<250 µg/g) approximately
268 around two and five years post diagnosis, respectively. Furthermore, FC4 (n=103;
269 ~10%), FC5 (n=67; ~6%) and FC6 (n=64; ~6%) capture relapsing and remitting
270 patterns of gastrointestinal inflammation. Finally, FC8 (n=194; ~19%) represented
271 individuals with consistently high FC values.

272

273 Associations with respect to FC cluster assignments

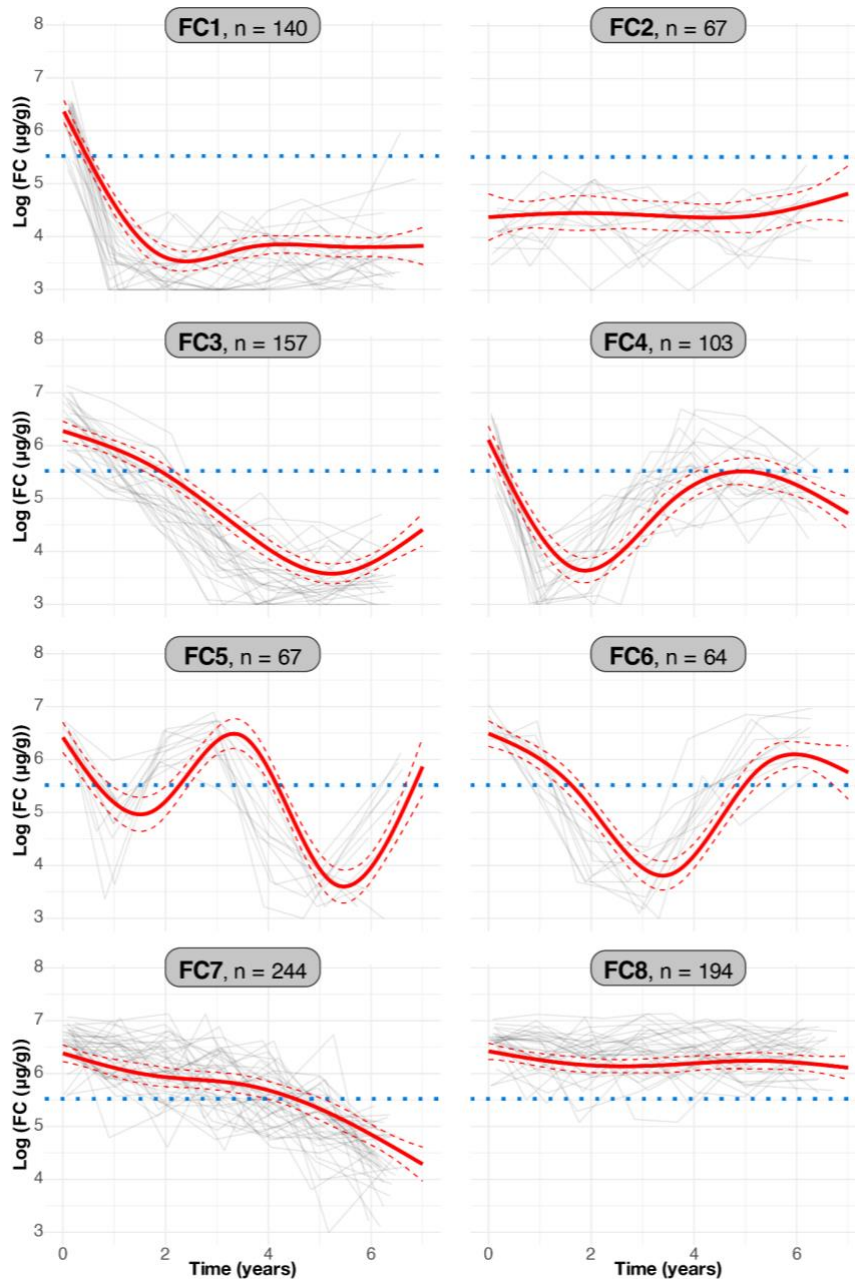
274 Associations with respect to age, sex and IBD type were first considered. Whilst the
275 effect of age and sex was not substantial ([Figure S8](#)), this was not the case for IBD
276 type ([Figure S9](#)). For example, IBDU and UC patients were less likely to be assigned
277 to FC6 (1.56% IBDU and 28.1% UC vs 11.4% and 37.3% respectively elsewhere).

278 A similar analysis was performed after stratifying by IBD type (UC and CD only) and
279 considering additional phenotyping ([Figures S10 - S16](#)). In most cases, effect sizes
280 were not statistically significant (in some cases this was due to low counts and small
281 cluster sizes). However, amongst CD patients, those without upper GI inflammation
282 were more likely to be assigned to FC1 or FC2 (2.4% and 3.03% L4 vs 18.1%
283 elsewhere). In UC, and to some extent CD, males were more likely to be assigned to
284 FC8 (72% male versus 49.7% elsewhere). Finally, UC patients with ulcerative proctitis
285 were found to be less likely to be assigned to FC3 (2.44% E1 versus 14.2%
286 elsewhere).

287 FC cluster assignment and advanced therapy usage

288 In total, 270 (49.6%) CD and 108 (28.4%) UC subjects received an advanced therapy
289 within the seven year observation period ([Table 1](#)). Overall AT rates and the
290 distribution of time to first AT were not homogeneous across clusters ([Figure 3](#)). For
291 example, whilst AT prescription rates in FC1 largely matched the overall FC cohort,
292 prescriptions were generally earlier in this cluster, especially in CD patients. It was
293 noteworthy that patients in FC8, with consistently high FC levels and later onset of AT,

294 had cumulative AT rates of 56.8% in CD and 37.9% in UC by the end of the seven
295 year observation period.



296

297

298 *Figure 2. Cluster trajectories obtained from LCMM assuming eight clusters fitted to FC data (log-*

299 *transformed). Red lines indicate predicted mean cluster profiles with 95% confidence intervals. The*

300 *blue dotted lines indicate log(250µg/g). For visualisation purposes, pseudo subject-specific*

301 *trajectories have been generated by amalgamating observations from randomly selected groups of six*

302 *subjects. Clusters are ordered from lowest (FC1) to highest (FC8) cumulative inflammatory burden.*

303 *Cluster sizes are shown as panel titles.*

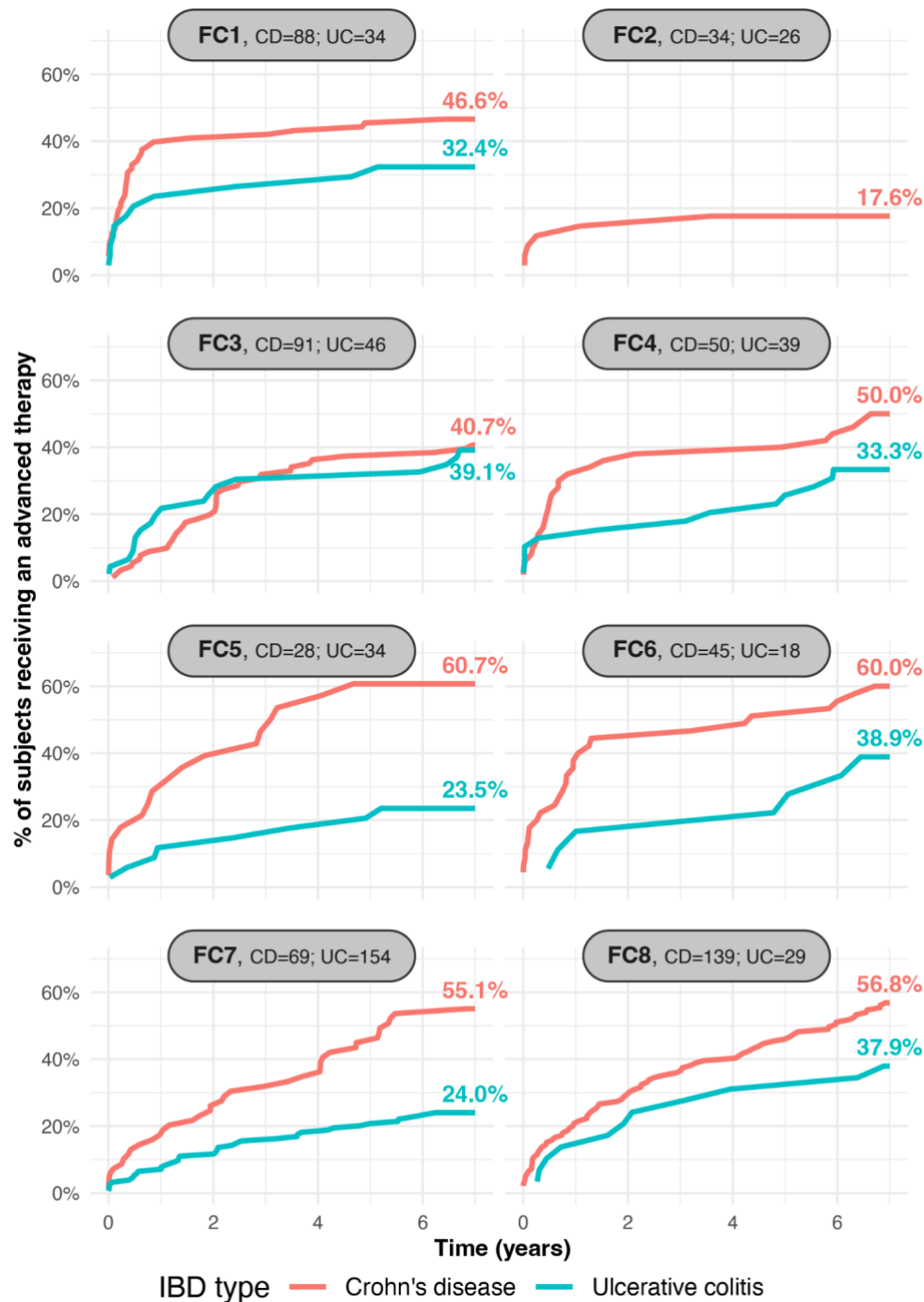
304 Modelling of CRP trajectories

305 AIC and BIC both suggested the 8-cluster model was the most appropriate ([Table S4](#)).
306 Visual inspection also supported this finding as the 9-cluster model did not identify new
307 trajectories when compared to the 8-cluster model, producing two trajectories with
308 consistently low CRP ([Figure S8](#)). In contrast, the 7-cluster model ([Figure S9](#)) lacks
309 one of the clinically interesting trajectories, characterised by an initially elevated CRP
310 which then decreases to slightly above biochemical remission after one year, when
311 compared to the 8-cluster model.

312 [Figure 4](#) presents exemplar cluster profiles for the 8-cluster model. Over a third of
313 subjects (n=702; ~38%) were assigned to CRP1 which was defined by consistently
314 low CRP. CRP2 (n=225; ~12%) was characterised by high CRP at diagnosis which
315 rapidly decreased shortly thereafter remaining low. CRP3 (n=51; ~3%) and CRP4
316 (n=60; ~3%) are both small clusters with the former described by low CRP until the
317 last year of follow-up and the latter presenting as low inflammation within the first year
318 of diagnosis before increasing until the third year where the inflammation then
319 decreases again. CRP5 (n=110; 6%) is characterised by elevated CRP at diagnosis
320 which then decreases gradually over time. CRP6 (n=434; 24%) consists of trajectories
321 which are elevated at diagnosis which then falls slightly for the first two years after
322 diagnosis, remaining elevated across the remaining duration of follow-up. CRP8
323 (n=172; 9%) is consistently elevated and does not change over time.

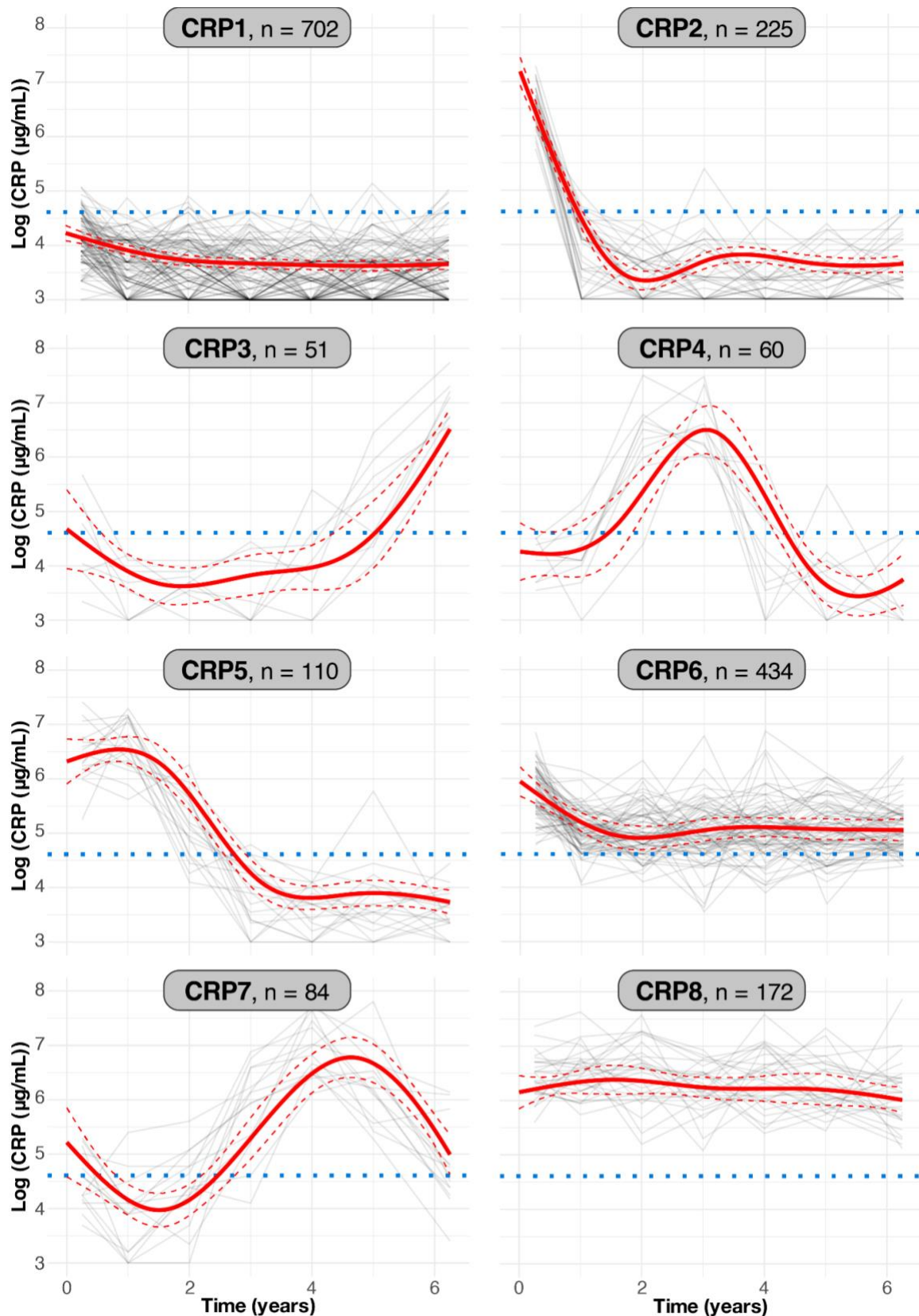
324 Associations with CRP cluster assignments

325 [Figure S19](#) and [S20](#) visualise the distribution of age, sex and IBD type within each
326 CRP cluster. Older patients were more likely to be assigned to a CRP cluster with
327 higher cumulative inflammatory burden. IBD type was not evenly distributed among
328 CRP clusters, with CRP1, CRP3, CRP4 and CRP7 enriched for UC patients (59.3%,
329 56.8%, 61.7% and 72.6% UC vs 32.3% elsewhere). Amongst CD patients, higher
330 smoking rates were generally observed for CRP clusters with higher inflammatory
331 burden (e.g. 26.9% in CRP1, 54.0% in CRP8; [Figure S21](#)), but there were not
332 substantial differences when considering Montreal location and behaviour, or upper
333 gastrointestinal inflammation ([Figures S22 - S24](#)). AT prescribing patterns in CRP
334 clusters are shown in [Figure S25](#).



335
336
337
338
339
340
341

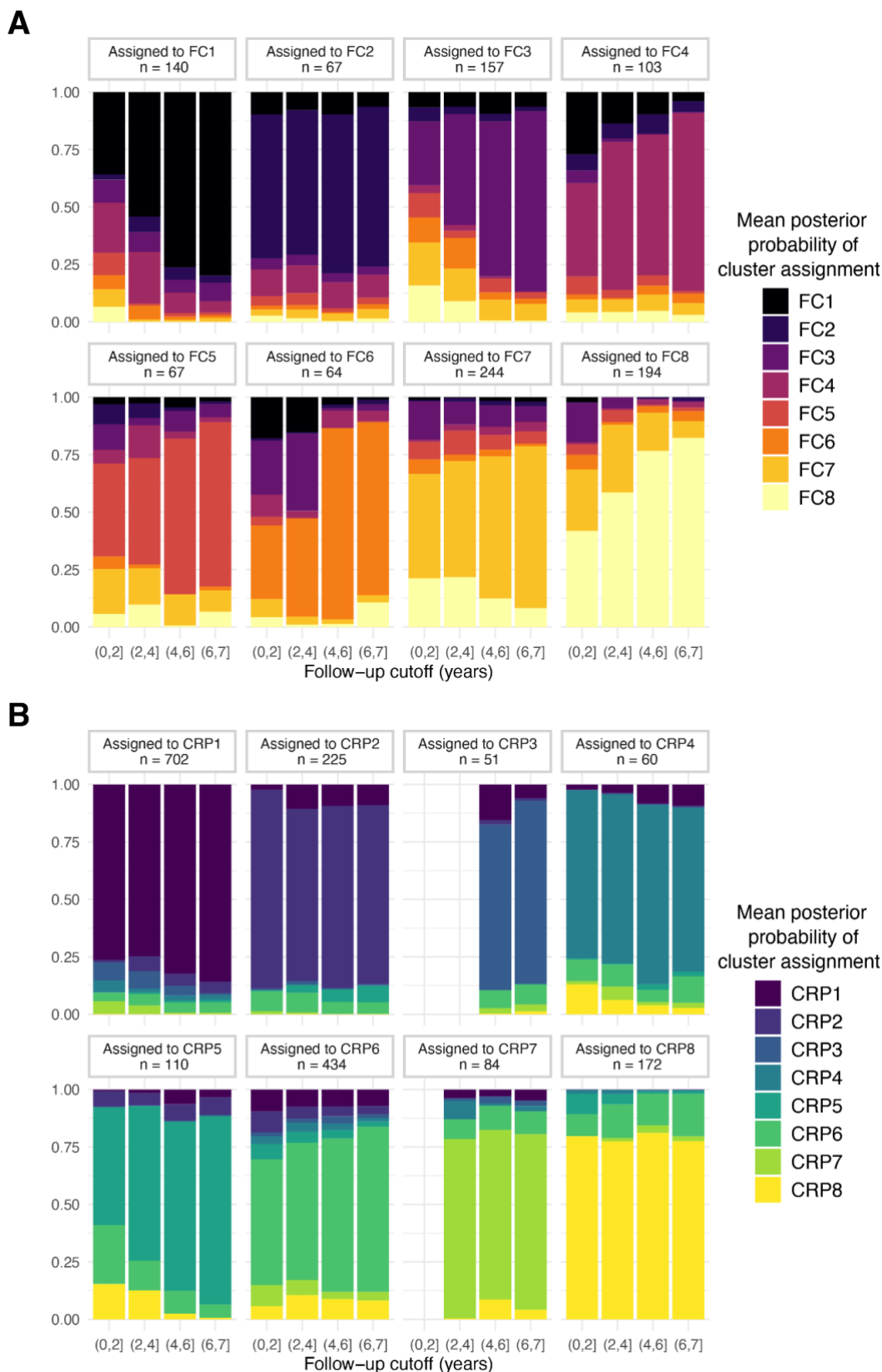
Figure 3. FC cluster-specific cumulative distribution for first-line advanced therapy prescribing for Crohn's disease (red) and ulcerative colitis (teal) subjects. Clusters are ordered from lowest (FC1) to highest (FC8) cumulative inflammatory burden. The number of CD and UC subjects present in each cluster is displayed as panel titles. Total advance therapy prescribing (as a percentage of the corresponding group) within seven years from diagnosis is shown next to each distribution curve. Curves which would describe fewer than five subjects are not shown.



342
343
344
345
346

Figure 4. Cluster trajectories obtained from LCMM assuming eight clusters fitted to processed CRP data (log-transformed). Red lines indicate predicted mean cluster profiles with 95% confidence intervals. The blue dotted lines indicate $\log(5\mu\text{g/mL})$. For visualisation purposes, pseudo subject-specific trajectories have been generated by amalgamating observations from randomly selected

347 groups of six subjects. Clusters are ordered from lowest (CRP1) to highest (CRP8) cumulative
 348 inflammatory burden. Cluster sizes are shown as panel titles.



349
 350 *Figure 5. Exploration of cluster assignment uncertainty for A) faecal calprotectin (FC) and B) CRP*
 351 *clusters. LCMM assigns individuals to the cluster with the highest estimated probability. For*

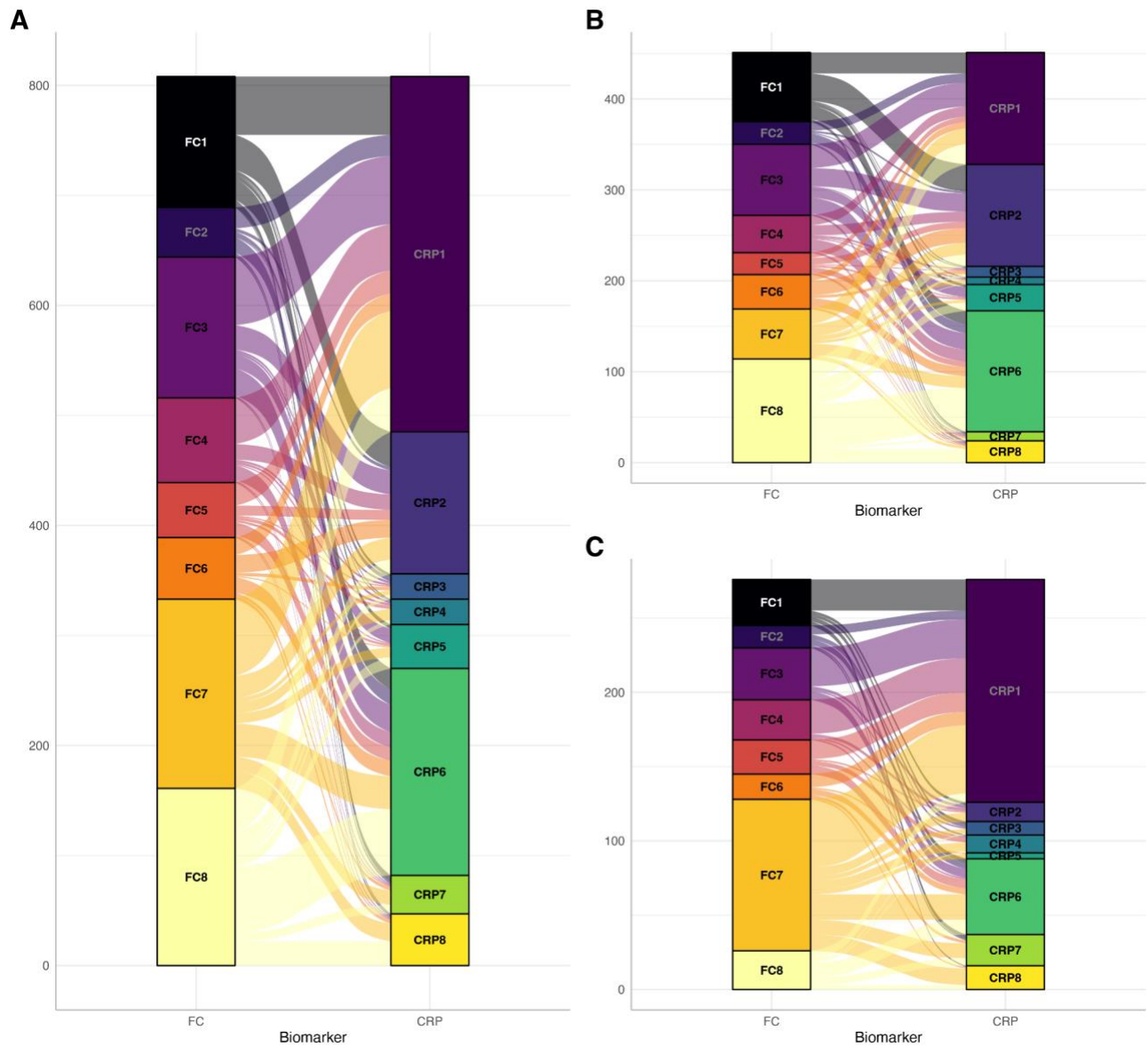
352 *individuals assigned to a given cluster, bars show the average probability of cluster assignment to*
353 *each possible cluster. Results are stratified according to follow-up length, defined as the time*
354 *difference between diagnosis and the last available biomarker measurement (FC or CRP for A) and*
355 *B), respectively). Clusters are ordered from lowest (FC1 and CRP1) to highest (FC8 and CRP8)*
356 *cumulative inflammatory burden, with adjacent clusters coloured sequentially in the plots for FC (black*
357 *to yellow) and CRP (blue to yellow).*

358 Uncertainty in cluster assignments

359 In the FC analysis, with the exception of FC2, cluster assignments were on average
360 more uncertain for subjects with a short follow-up ([Figure 5](#) (A)). This is particularly the
361 case for FC clusters that share similar earlier trends. For example, individuals
362 assigned to FC1 (rapid FC normalisation) had a low average probability of being
363 assigned to FC8 (consistently high FC) and vice-versa, even for those with a short
364 follow-up. This is not the case when comparing FC3 and FC6, both of which capture
365 similar FC trajectories within the first two years. Indeed, those assigned to FC6 with
366 less than two years of follow-up also have, on average, a high probability of being
367 assigned to FC3. On average, cluster assignments were less uncertain in the CRP
368 analysis, even for individuals with a short follow-up ([Figure 5](#) (B)). This is expected as
369 CRP clusters are associated with more distinct early trajectories.

370 Comparison of FC and CRP clustering

371 Overall, all FC clusters were well represented amongst the 808 subjects included in
372 both analyses (*overlap cohort*), but CRP8 was underrepresented (~27% of CRP8 was
373 in the overlap cohort vs ~46% elsewhere; [Figure S26](#)). When comparing FC and CRP
374 clustering in the overlap cohort, there was little agreement ([Figure 6](#) (A)). Whilst most
375 subjects in FC1 (71.6%) were also in CRP1 or CRP2, this relationship was not mirrored
376 as 81.2% of subjects in the latter two clusters were assigned to substantially different
377 FC clusters. However, CRP8 did overlap with elevated FC as the vast majority of
378 subjects in this cluster (80.8%) were assigned to either FC7 or FC8. For the 451 CD
379 subjects in the overlap cohort, largely similar patterns were observed ([Figure 6](#) (B)).
380 For the 276 UC subjects, a substantial proportion of FC7 (45.1%) were assigned to
381 CRP1 ([Figure 6](#) (C)), perhaps reflecting the characteristic where UC patients are less
382 likely to mount an abnormal CRP response than CD patients²¹.



383

384

385

386

387

388

Figure 6. Comparison between faecal calprotectin (FC) and processed CRP for models with chosen specification (three NCS) assuming eight clusters. Results are reported based on the overlap cohort, consisting of 808 subjects included in both the FC and CRP analysis. (A) all subjects; (B) Crohn's disease; and (C) ulcerative colitis. Each segment denotes the size of the cluster whilst the alluvial segments connecting the nodes visualises the number of subjects shared between clusters.

389

Discussion

390

391

392

393

We have characterised IBD behaviour using long-term longitudinal trends of objective inflammatory markers routinely collected for clinical care. Our model has uncovered, in a large IBD cohort, eight clusters with distinct inflammatory profiles based on FC and CRP, respectively. Our data highlights the heterogeneity of the disease course,

394 and present a novel approach for understanding real-world patterns of inflammatory
395 activity in IBD patients. For the first time, we are capturing the dynamic nature of the
396 disease in a more biologically nuanced way than traditional behaviour endpoints such
397 as treatment escalation, surgery and “Montreal progression”. Moreover, this
398 represents a marked shift from the traditional symptom-based behaviour profiles
399 exemplified by the IBSEN cohorts over a decade ago.^{9,10}

400

401 This study builds on our earlier proof-of-concept work, where we first demonstrated
402 the feasibility of using long-term individualised profiles of FC to cluster IBD patients
403 with CD.¹⁵ In our previous analysis we identified four distinct FC clusters: one cluster
404 with persistently high FC (non-remitters) and three clusters with different downward
405 longitudinal trends. Here, we expand upon this by considering a substantially larger
406 IBD cohort (FC cohort, n=1036; CRP cohort, n=1838), with longer follow-up, not
407 excluding patients based on indicators of disease severity, and also including patients
408 with UC or IBDU. In addition, we modelled CRP. This has generated results with
409 greater representativeness across IBD phenotypes, uncovering more granular
410 structure with eight distinct FC clusters rather than four. Whilst the modelling
411 suggested further partitioning of the FC data was possible ([Figure S5](#), [Figure S7 \(A\)](#)),
412 we selected the eight-cluster model as a parsimonious choice that captured the key
413 inflammatory patterns ([Figure 2](#)). Notably, the CRP data also partitioned into eight
414 distinct clusters. Together, the clusters broadly fall into four patterns of inflammatory
415 behaviour mirroring those recognised by gastroenterologists managing IBD patients
416 (i) rapid remitters (FC1 and CRP2), (ii) delayed remitters (FC3, FC7 and CRP5), (iii)
417 relapsing-remitters (FC4-6 and CRP4 and CRP7), and (iv) non-remitters (FC8 and
418 CRP6 and CRP8). These classifications provide new insights into the inflammatory
419 course of IBD patients.

420

421 We observed broadly poor agreement between FC and CRP clusters, although there
422 was overlap amongst those at the varying ends of the inflammatory spectrum with FC1
423 and FC2 correlating with CRP1 and CRP2 (rapid remitters with low cumulative
424 inflammatory burden), and FC7 and FC8 correlating with CRP6-8 (non-remitters with
425 high cumulative inflammatory burdens). Although, the lack of overlap between the two
426 is not surprising. CRP is a marker of systemic inflammation, whilst FC is more specific
427 for detecting inflammation at a mucosal level. Hence, why both biomarkers are

428 complimentary when monitoring patients with IBD. Studies have also shown that a
429 proportion of IBD patients will have lower CRP values at diagnosis,²² as is seen in
430 CRP1 which is significantly enriched for UC cases.

431

432 We observed several important observations regarding cluster assignment. All IBD
433 subtypes featured in each cluster, however cluster assignment was unevenly
434 distributed across CD, UC and IBDU (Figures [S9](#) and [S20](#)). In CD, although patients
435 with L4 disease were less represented in FC1 and FC2 there was no association with
436 ileal versus colonic disease location. Males were slightly overrepresented in the FC8
437 cluster, which is characterised by persistently elevated values. Interestingly, in the
438 recent SEXEII study, they observed male patients with UC were more likely to have
439 extensive colonic involvement and abdominal surgery, which may account for this
440 finding.²³ CRP cluster membership was also associated with smoking and older age,
441 with both more likely to have higher inflammatory burdens.

442

443 Multiple lines of evidence, including the recent PROFILE study,²⁴ have clearly
444 demonstrated improved disease control with and outcomes in Crohn's patients
445 receiving early advanced therapy. As such, we anticipated that the biggest driver of
446 inflammatory patterns over time would be advanced therapies and that this effect
447 would be more pronounced in CD versus UC especially given the era of our cohort.
448 Indeed, rates of advanced therapy use were not homogenous across clusters or IBD
449 subtypes. Overall, in the FC cohort, advanced therapies were used in 49.6% of CD
450 patients of which 47.7% started AT in the first year. In FC1, similar rates of advanced
451 therapies were used for Crohn's patients, however they were used earlier, suggesting
452 their positive benefit in rapidly inducing and maintaining remission. Rates of advanced
453 therapy prescriptions for patients with CD in FC8 (persistently high levels of
454 inflammatory behaviour) were similar, but started later in the disease course, which
455 may have negatively affected the ability to bring about remission of disease. This
456 cluster may also represent a more refractory group of patients, with a higher risk
457 phenotype. Whilst this may provide additional support for the use of early advanced
458 therapy, a causal interpretation of these effects is not possible in this study, which is
459 based on observational data. Additional work with alternative cohorts where treatment
460 assignment is randomised is planned.

461 Our study also highlights the importance of using a probabilistic approach to account
462 for uncertainty in cluster assignments. Indeed, we observed higher uncertainty for
463 subjects with a shorter longitudinal follow-up, particularly for FC clusters (Figure 5). In
464 such cases, we cannot confidently assign individuals to a specific cluster. Instead,
465 cluster assignment probabilities are sometimes evenly split across multiple clusters,
466 mostly between those with similar earlier behaviour and inflammatory burdens. This
467 effect is less prominent in CRP cluster assignments, partly due to the more distinct
468 early trajectories observed across CRP clusters. As such, we anticipate that a
469 multivariate approach which simultaneously considers other biomarkers of disease
470 activity, such as haemoglobin, albumin, and platelet count, may further increase the
471 robustness of cluster assignments. Such analysis may also consider pre-diagnostic
472 biomarker measurements, following the recent observations in Danish registry data,²⁵
473 as well as metabolomics, genetics or microbiome data to inform cluster assignments.
474 Critically, this study is limited to data generated in a single health board in Scotland.
475 As such, independent validation of the identified longitudinal clusters will be necessary
476 before clinical implementation and to better understand the associations between
477 cluster assignment and disease phenotyping. Furthermore, there are limitations
478 associated with the use of observational data. Beyond advanced therapy use, the
479 frequency and amount of biomarker measurements is likely to be higher for those with
480 a more severe disease, and very mild cases may be excluded from our cohort.
481 Moreover, FC and CRP clusters cannot be directly used in a prognostic way. Indeed,
482 future work is needed to assess associations between clusters and IBD related
483 complications (such as steroid use, hospitalisations and surgery) but also non-
484 conventional complications related to a high cumulative inflammatory burden, such as
485 major cardiovascular adverse events, neuropsychiatric illness, and malignancy. Such
486 analyses will ultimately support the development of a low cost clinical support tool to
487 help deliver precision medicine to patients with IBD.

488 Classifying patients by their inflammatory behaviour may better inform therapy
489 decisions, including timing of advanced therapy, as well as monitoring and follow-up
490 requirements. This is a paradigm shift in thinking about disease behaviour compared
491 with the previous symptom based profiles first reported by the IBSEN cohorts.
492 Moreover, this approach - rooted in data that is widely available in clinical settings²⁶
493 and probabilistic modelling- paves the way for predictive analytics integrated into a

494 clinical support tool for population wide risk stratification and individual patient level
495 prognostication and treatment.

496 Data sharing statement

497 As the data collected for this study has been derived from unconsented patient data,
498 it is not possible to share subject-level data with external entities. Detailed summary
499 level data is available online at <https://vallejosgroup.github.io/Lothian-IBDR>. The
500 code used to conduct the analysis is also publicly available
501 (<https://github.com/VallejosGroup/Lothian-IBDR>).

502 Author contributions

503 CAV, CWL, and NCC were involved in conceptualising the study. CRB, SO, ATE, GRJ,
504 and NP curated the data. NCC and CAV implemented computer code, tested existing
505 code components, and conducted the formal analysis and visualisation. The original
506 draft was written by NCC, NP, ATE, CMR, CWL and CAV with all authors involved in
507 reviewing and editing the manuscript. CWL and CAV provided supervisory support.

508 Competing interests

509 NP has served as a speaker for Janssen, Takeda and Pfizer. BG has acted as
510 consultant to Galapagos and Abbvie and as speaker for Abbvie, Jansen, Takeda,
511 Pfizer and Galapagos. G-RJ has served as a speaker for Takeda, Janssen, Abbvie,
512 Fresenius and Ferring. CWL has acted as a speaker and/or consultant to AbbVie,
513 Janssen, Takeda, Pfizer, Galapagos, GSK, Gilead, Vifor Pharma, Ferring, Dr Falk,
514 BMS, Boehringer Ingelheim, Eli Lilly, Merck, Novartis, Sandoz, Celltrion, Cellgene,
515 Amgen, Samsung Bioepis, Fresenius Kabi, Tillotts, Kuma Health, Trellus Health and
516 Iterative Health. None of the other authors report any conflicts of interest.

517 Funding

518 CWL is funded by a UKRI (UK Research and Innovation) Future Leaders Fellowship
519 'Predicting outcomes in IBD' (MR/S034919/1). G-RJ is funded by a Wellcome Trust
520 Clinical Research Career Development Fellowship. NC-C was partially supported by
521 the Medical Research Council and The University of Edinburgh via a Precision
522 Medicine PhD studentship (MR/N013166/1).

523 References

524

- 525 1. Jones GR, Lyons M, Plevris N, et al. IBD prevalence in Lothian, Scotland,
526 derived by capture–recapture methodology. *Gut*. 2019;68(11):1953-1960.
527 doi:10.1136/gutjnl-2019-318936
- 528 2. Hamilton B, Green H, Heerasing N, et al. Incidence and prevalence of
529 inflammatory bowel disease in Devon, UK. *Frontline Gastroenterol*.
530 2021;12(6):461-470. doi:10.1136/flgastro-2019-101369
- 531 3. Cushing K, Higgins PDR. Management of Crohn disease: A review. *JAMA*.
532 2021;325(1):69. doi:10.1001/jama.2020.18936
- 533 4. Gros B, Kaplan GG. Ulcerative colitis in adults: A review. *JAMA*.
534 2023;330(10):951. doi:10.1001/jama.2023.15389
- 535 5. Zhou RW, Harpaz N, Itzkowitz SH, Parsons RE. Molecular mechanisms in colitis-
536 associated colorectal cancer. *Oncogenesis*. 2023;12(1):48. doi:10.1038/s41389-
537 023-00492-0
- 538 6. Kennedy NA, Jones GR, Plevris N, Patenden R, Arnott ID, Lees CW. Association
539 between level of fecal calprotectin and progression of Crohn’s disease. *Clin*
540 *Gastroenterol Hepatol*. 2019;17(11):2269-2276.e4.
541 doi:10.1016/j.cgh.2019.02.017
- 542 7. Plevris N, Fulforth J, Lyons M, et al. Normalization of fecal calprotectin within 12
543 months of diagnosis is associated with reduced risk of disease progression in
544 patients with Crohn’s disease. *Clin Gastroenterol Hepatol*. 2021;19(9):1835-
545 1844.e6. doi:10.1016/j.cgh.2020.08.022
- 546 8. Verstockt B, Noor NM, Marigorta UM, et al. Results of the Seventh Scientific
547 Workshop of ECCO: Precision medicine in IBD—Disease outcome and response
548 to therapy. *J Crohns Colitis*. 2021;15(9):1431-1442. doi:10.1093/ecco-jcc/jjab050
- 549 9. Solberg IC, Vatn MH, Høie O, et al. Clinical course in Crohn’s disease: Results of
550 a Norwegian population-based ten-year follow-up study. *Clin Gastroenterol*
551 *Hepatol*. 2007;5(12):1430-1438. doi:10.1016/j.cgh.2007.09.002
- 552 10. Solberg IC, Lygren I, Jahnsen J, et al. Clinical course during the first 10 years of
553 ulcerative colitis: Results from a population-based inception cohort (IBSEN
554 Study). *Scand J Gastroenterol*. 2009;44(4):431-440.
555 doi:10.1080/00365520802600961
- 556 11. Peyrin-Biroulet L, Reinisch W, Colombel JF, et al. Clinical disease activity, C-
557 reactive protein normalisation and mucosal healing in Crohn’s disease in the
558 SONIC trial. *Gut*. 2014;63(1):88-95. doi:10.1136/gutjnl-2013-304984
- 559 12. Silverberg MS, Satsangi J, Ahmad T, et al. Toward an integrated clinical,
560 molecular and serological classification of inflammatory bowel disease: Report of

- 561 a working party of the 2005 Montreal World Congress of Gastroenterology. *Can J*
562 *Gastroenterol Hepatol.* 2005;19:5A-36A. doi:10.1155/2005/269076
- 563 13. Lennard-Jones JE. Classification of inflammatory bowel disease. *Scand J*
564 *Gastroenterol.* 1989;24(sup170):2-6. doi:10.3109/00365528909091339
- 565 14. Sorlie P, Wei GS. Population-based cohort studies: Still relevant? *J Am Coll*
566 *Cardiol.* 2011;58(19):2010-2013. doi:10.1016/j.jacc.2011.08.020
- 567 15. Constantine-Cooke N, Monterrubio-Gómez K, Plevris N, et al. Longitudinal fecal
568 calprotectin profiles characterize disease course heterogeneity in Crohn's
569 disease. *Clin Gastroenterol Hepatol.* 2023;21(11):2918-2927.e6.
570 doi:10.1016/j.cgh.2023.03.026
- 571 16. Proust-Lima C, Philipps V, Liqueur B. Estimation of extended mixed models using
572 latent classes and latent processes: The R package lcmm. *J Stat Softw.*
573 2017;78(2):1-56. doi:10.18637/jss.v078.i02
- 574 17. Stoica P, Selen Y. Model-order selection: A review of information criterion rules.
575 *IEEE Signal Process Mag.* 2004;21(4):36-47. doi:10.1109/MSP.2004.1311138
- 576 18. Proust-Lima C, Philipps V, Diakite A, Liqueur B. lcmm: extended mixed models
577 using latent classes and latent processes. Published online 2021. [https://cran.r-](https://cran.r-project.org/package=lcmm)
578 [project.org/package=lcmm](https://cran.r-project.org/package=lcmm)
- 579 19. Brunson JC. ggalluvial: layered grammar for alluvial plots. *J Open Source Softw.*
580 2020;5(49):2017. doi:10.21105/joss.02017
- 581 20. Constantine-Cooke N. datefixR: fix really messy dates in R. Published online
582 2024. doi:10.5281/zenodo.5655311
- 583 21. Clough J, Colwill M, Poullis A, Pollok R, Patel K, Honap S. Biomarkers in
584 inflammatory bowel disease: A practical guide. *Ther Adv Gastroenterol.*
585 2024;17:17562848241251600. doi:10.1177/17562848241251600
- 586 22. Henriksen M, Jahnsen J, Lygren I, et al. C-reactive protein: A predictive factor
587 and marker of inflammation in inflammatory bowel disease. Results from a
588 prospective population-based study. *Gut.* 2008;57(11):1518-1523.
589 doi:10.1136/gut.2007.146357
- 590 23. Gargallo-Puyuelo CJ, Ricart E, Iglesias E, et al. Sex-related differences in the
591 phenotype and course of inflammatory bowel disease: SEXEII study of ENEIDA.
592 *Clin Gastroenterol Hepatol.* 2024;22(11):2280-2290.
593 doi:10.1016/j.cgh.2024.05.013
- 594 24. Noor NM, Lee JC, Bond S, et al. A biomarker-stratified comparison of top-down
595 versus accelerated step-up treatment strategies for patients with newly
596 diagnosed Crohn's disease (PROFILE): A multicentre, open-label randomised
597 controlled trial. *Lancet Gastroenterol Hepatol.* 2024;9(5):415-427.
598 doi:10.1016/S2468-1253(24)00034-7

- 599 25. Vestergaard MV, Allin KH, Poulsen GJ, Lee JC, Jess T. Characterizing the pre-
600 clinical phase of inflammatory bowel disease. *Cell Rep Med*. 2023;4(11):101263.
601 doi:10.1016/j.xcrm.2023.101263
- 602 26. Markowitz F. All models are wrong and yours are useless: Making clinical
603 prediction models impactful for patients. *Npj Precis Oncol*. 2024;8(1):54.
604 doi:10.1038/s41698-024-00553-6
- 605

606 Supplemental display items

607 Table of contents

608 Supplemental figures

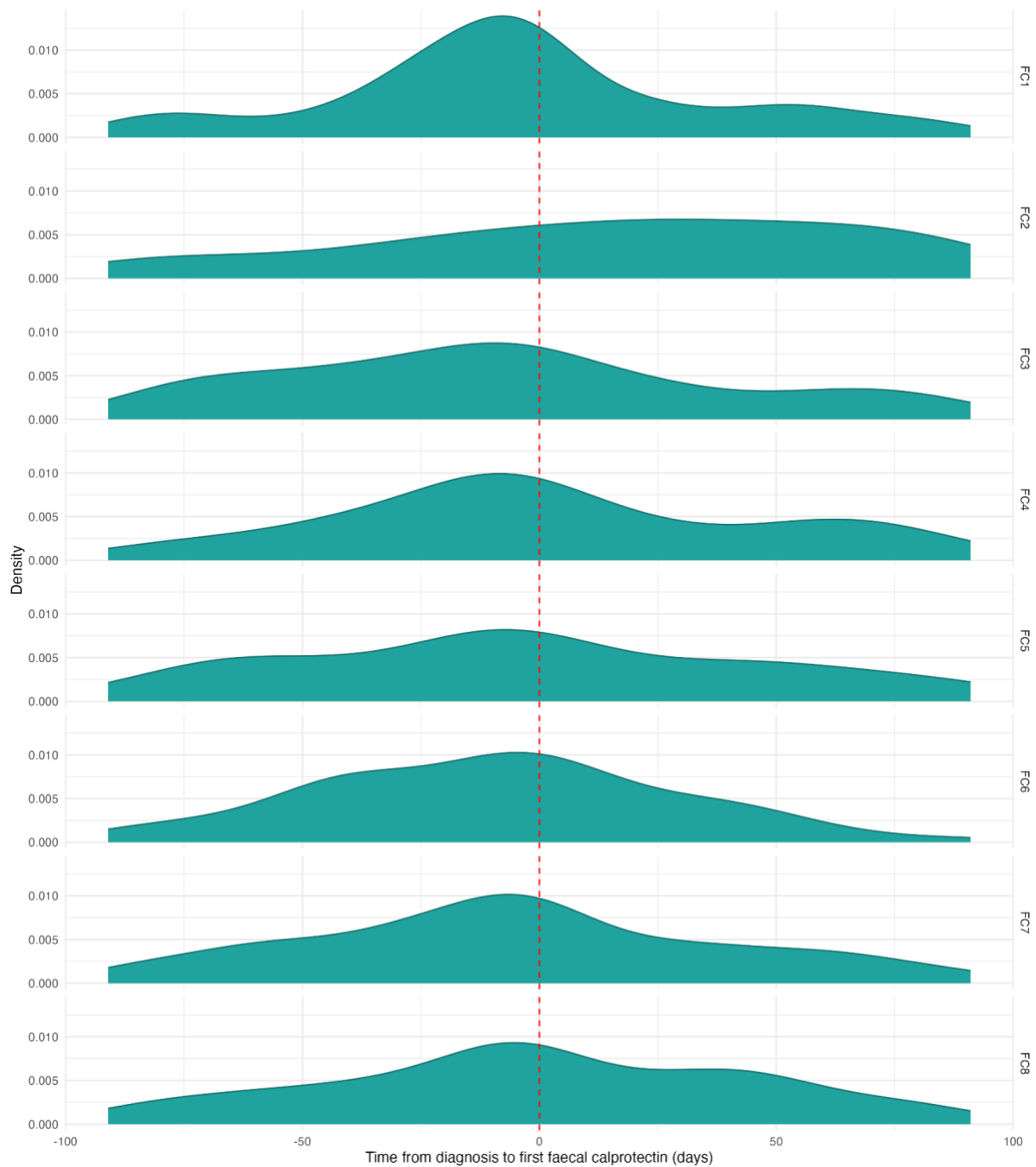
- 609 ● [Figure S1](#). Distribution of observation times for diagnostic FC
- 610 ● [Figure S2](#). Distribution of observation times for diagnostic CRP
- 611 ● [Figure S3](#). Illustration of how biomarker (faecal calprotectin or CRP)
- 612 observation times were adjusted based on time of diagnostic biomarker
- 613 observation
- 614 ● [Figure S4](#). Distribution of diagnostic biomarker measurements across the
- 615 study cohort
- 616 ● [Figure S5](#). Cluster trajectories obtained from LCMM assuming ten clusters
- 617 fitted to FC data
- 618 ● [Figure S6](#). Cluster trajectories obtained from LCMM assuming nine clusters
- 619 fitted to FC data
- 620 ● [Figure S7](#). Alluvial plot visualising cluster assignment as the number of
- 621 assumed clusters increases
- 622 ● **Associations with FC cluster membership**
- 623 ○ [Figure S8](#). Age and sex
- 624 ○ [Figure S9](#). IBD type
- 625 ○ [Figure S10](#). Smoking for CD subjects
- 626 ○ [Figure S11](#). Montreal location for CD subjects
- 627 ○ [Figure S12](#). L4 for CD subjects
- 628 ○ [Figure S13](#). Montreal behaviour for CD subjects
- 629 ○ [Figure S14](#). Perianal disease for CD subjects
- 630 ○ [Figure S15](#). Smoking for UC subjects
- 631 ○ [Figure S16](#). Montreal extent for UC subjects
- 632 ● [Figure S17](#). Cluster trajectories obtained from model assuming nine clusters
- 633 fitted to CRP data
- 634 ● [Figure S18](#). Cluster trajectories obtained from model assuming seven clusters
- 635 fitted to CRP data
- 636 ● **Associations with CRP cluster membership**

- 637 ○ [Figure S19](#). Age and sex
- 638 ○ [Figure S20](#). IBD type
- 639 ○ [Figure S21](#). Smoking for CD subjects
- 640 ○ [Figure S22](#). Montreal location for CD subjects
- 641 ○ [Figure S23](#). L4 for CD subjects
- 642 ○ [Figure S24](#). Montreal behaviour for CD subjects
- 643 ● [Figure S25](#). Time to first-line advanced therapy by CRP cluster assignment
- 644 ● [Figure S26](#). Proportion of individuals included in the overlap cohort by FC and
- 645 CRP cluster assignment

646 Supplemental tables

- 647 ● [Table S1](#). Model statistics for models fitted to FC data
- 648 ● [Table S2](#). Model statistics for models fitted to CRP data

649 Supplemental figures



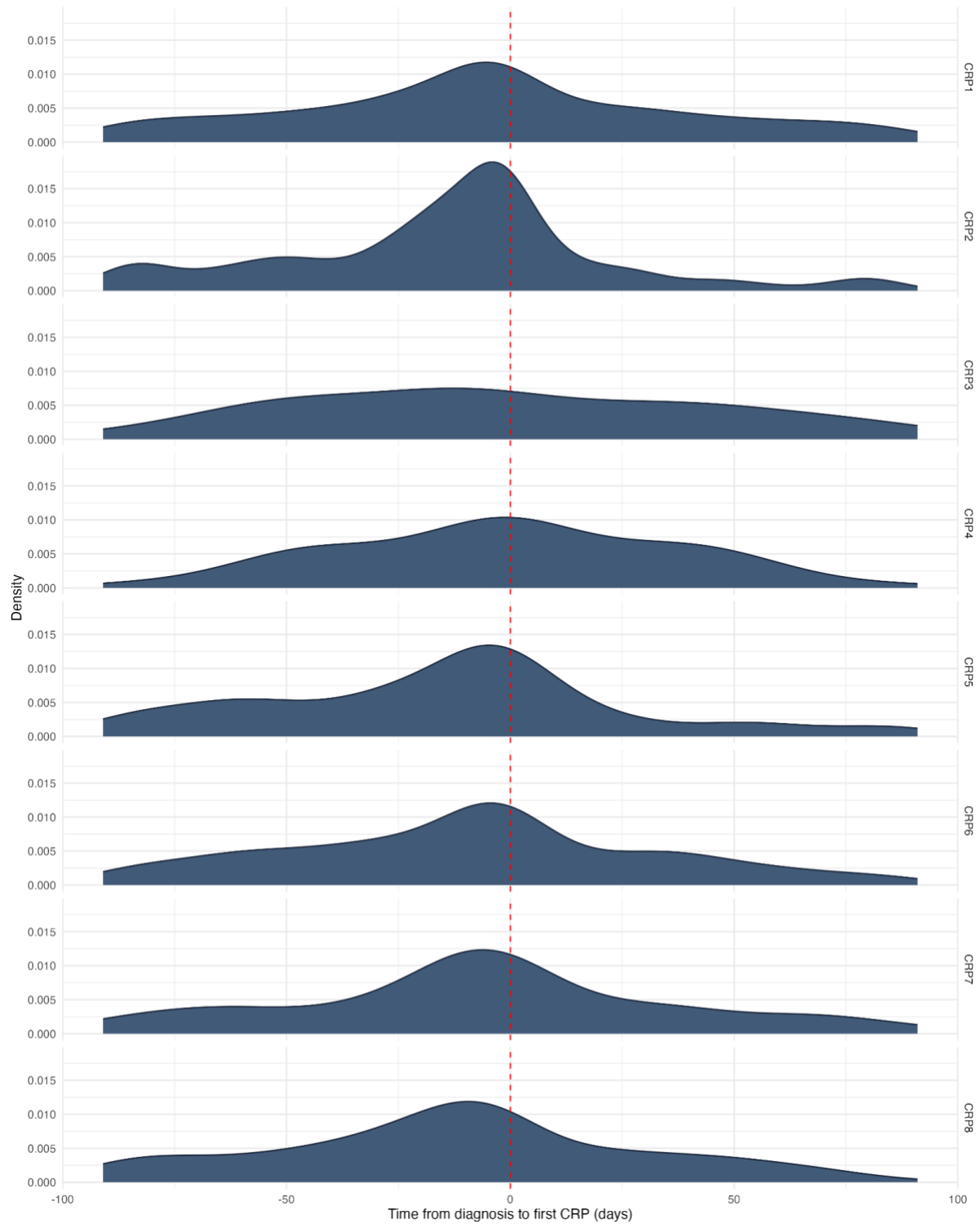
650

651

652

653

Figure S1. Distribution of observation times for diagnostic faecal calprotectin (FC) relative to reported date of diagnosis for the study cohort. Stratified by FC cluster assignment. Diagnostic FC was defined as the first FC test within ± 90 days of diagnosis.



654

655

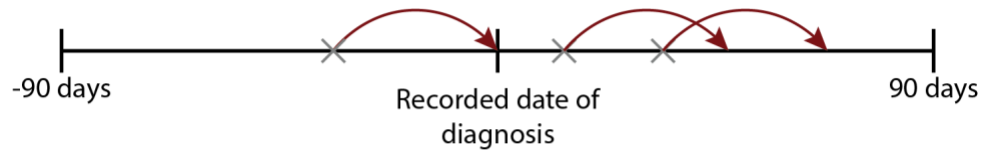
656

657

Figure S2. Distribution of observation times for diagnostic C-reactive protein (CRP) relative to reported date of diagnosis for the study cohort. Stratified by CRP cluster assignment. Diagnostic CRP was defined as the first CRP test within ± 90 days of diagnosis.

Scenario 1:

First biomarker measurement within 90 days of reported date of diagnosis is *before* diagnosis



Biomarker observations are re-timed by the same amount so the first observation now corresponds to diagnosis

Scenario 2:

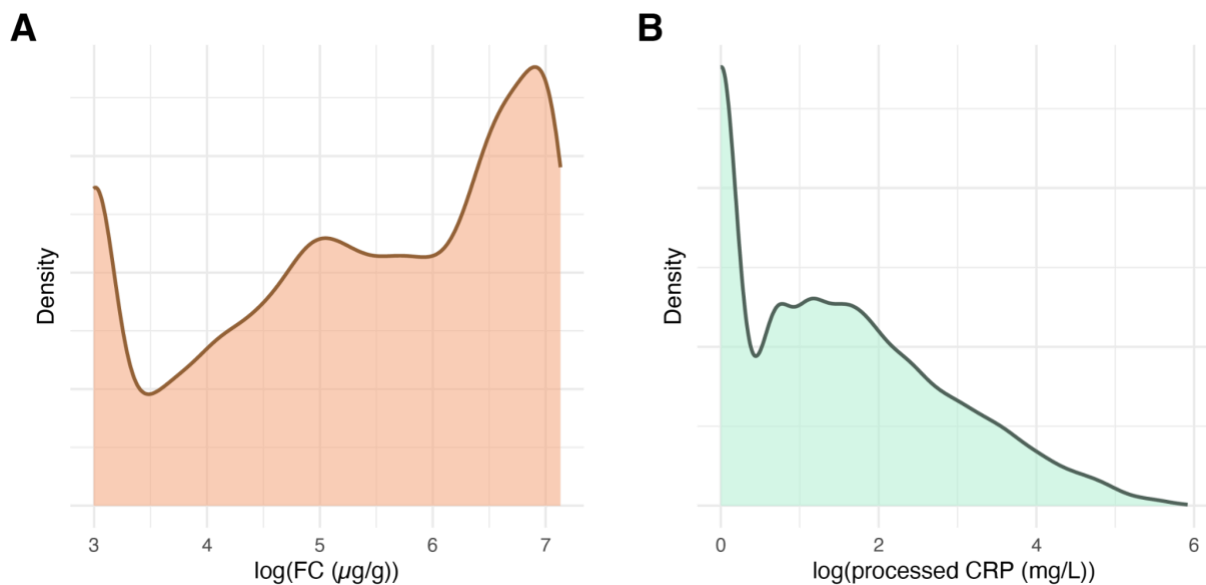
First biomarker measurement within 90 days of reported date of diagnosis is *after* diagnosis



Biomarker observations are not re-timed

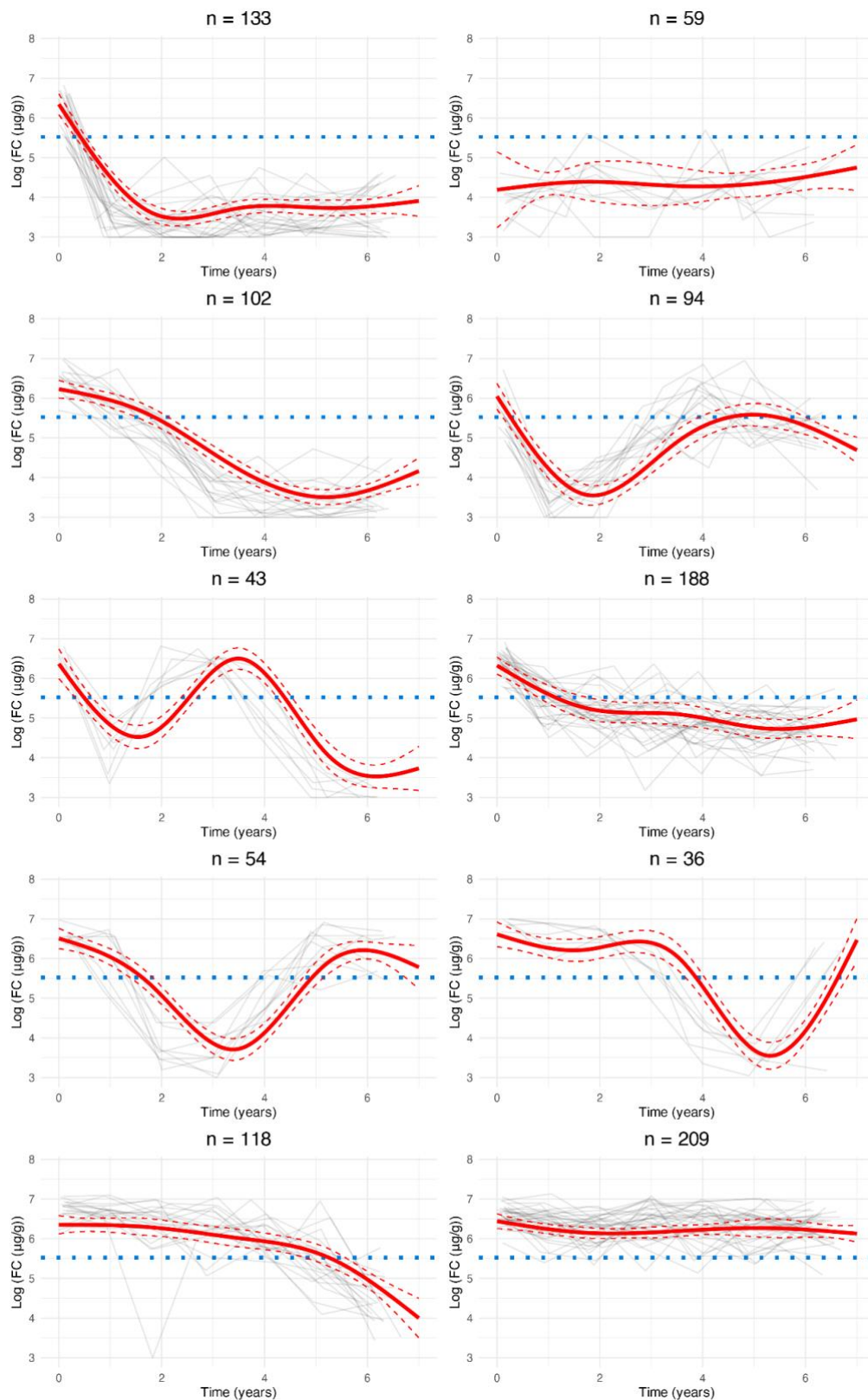
658
659
660
661

Figure S3. Illustration of how biomarker (faecal calprotectin or CRP) observation times were adjusted depending on if the diagnostic observation was before or after the date of diagnosis recorded in electronic health records.



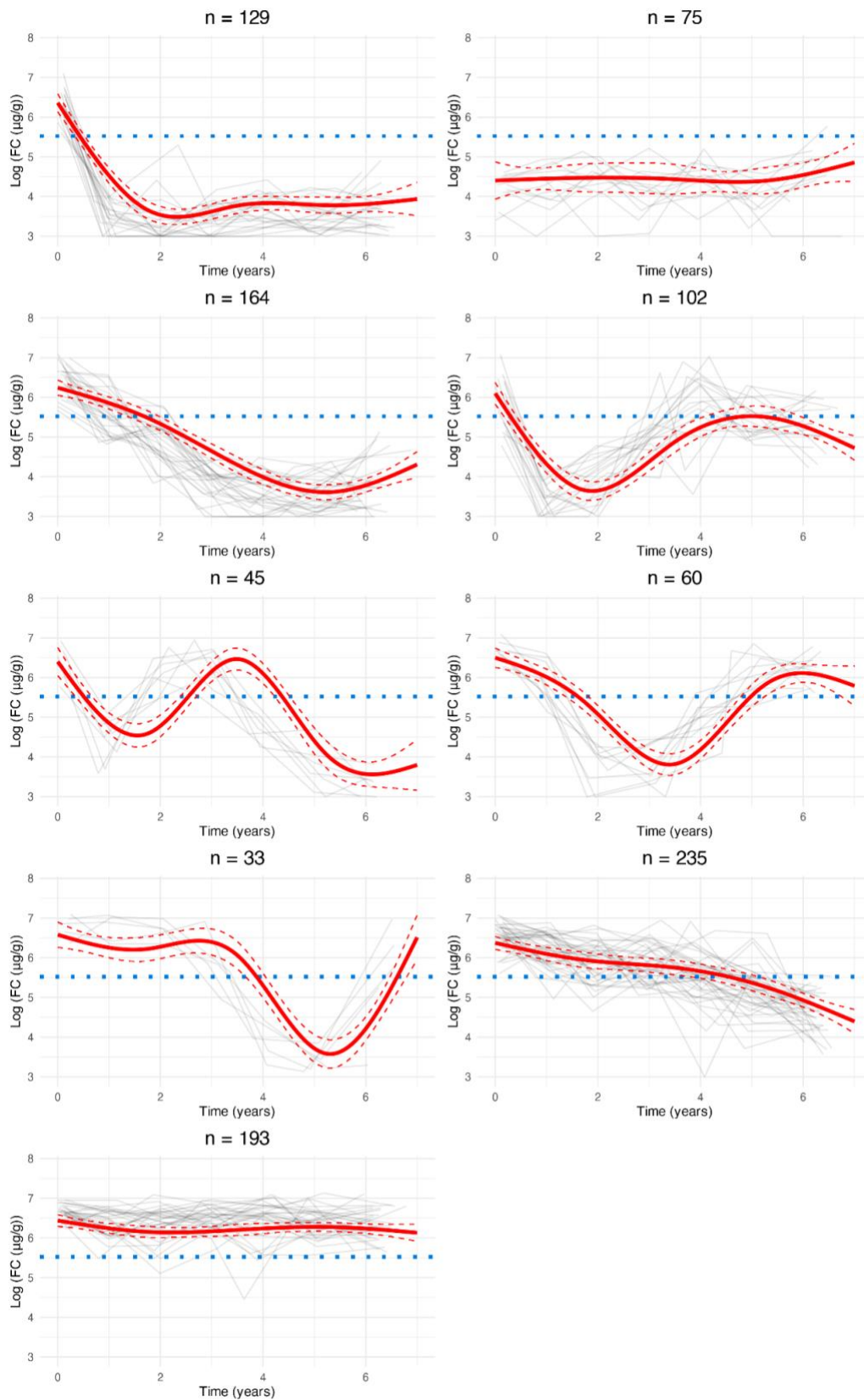
662
663
664
665

Figure S4. Distribution of diagnostic biomarker measurements across the study cohort. (A) faecal calprotectin after applying a logarithmic transformation; (B) pre-processed (grouped into time intervals with the median used for multiple measurements) CRP after logarithmic transformation.



666
667
668
669
670

Figure S5. Cluster trajectories obtained from LCMM assuming ten clusters fitted to faecal calprotectin data. Red lines indicate predicted mean cluster profiles with 95% confidence intervals. Dotted horizontal lines indicate $\log(250\mu\text{g/g})$. For visualisation purposes, pseudo subject-specific trajectories have been generated by amalgamating observations from groups of six subjects.



671

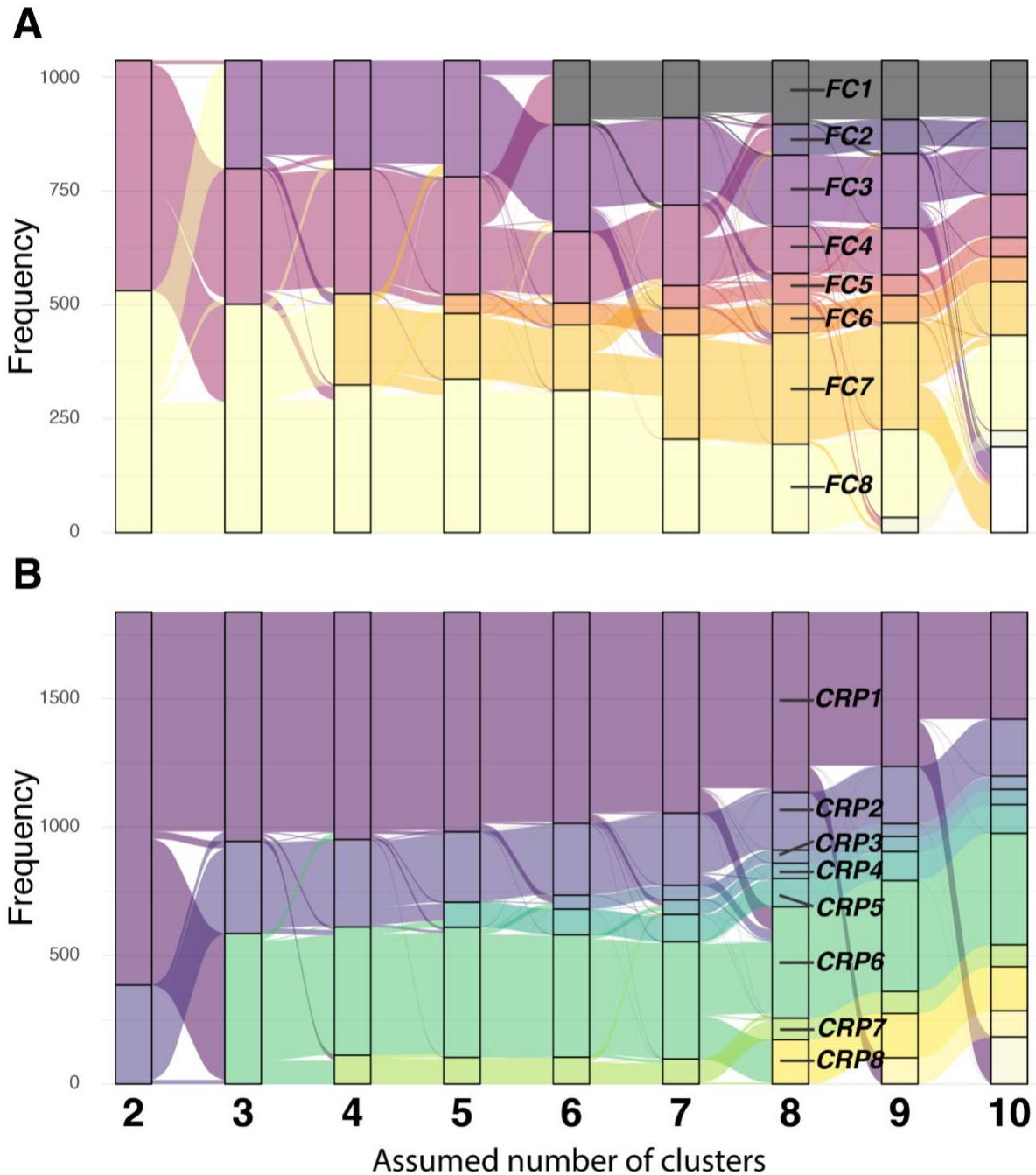
672

673

674

675

Figure S6. Cluster trajectories obtained from LCMM assuming nine clusters fitted to faecal calprotectin data. Red lines indicate predicted mean cluster profiles with 95% confidence intervals. Dotted horizontal lines indicate $\log(250\mu\text{g/g})$. For visualisation purposes, pseudo subject-specific trajectories have been generated by amalgamating observations from groups of six subjects.



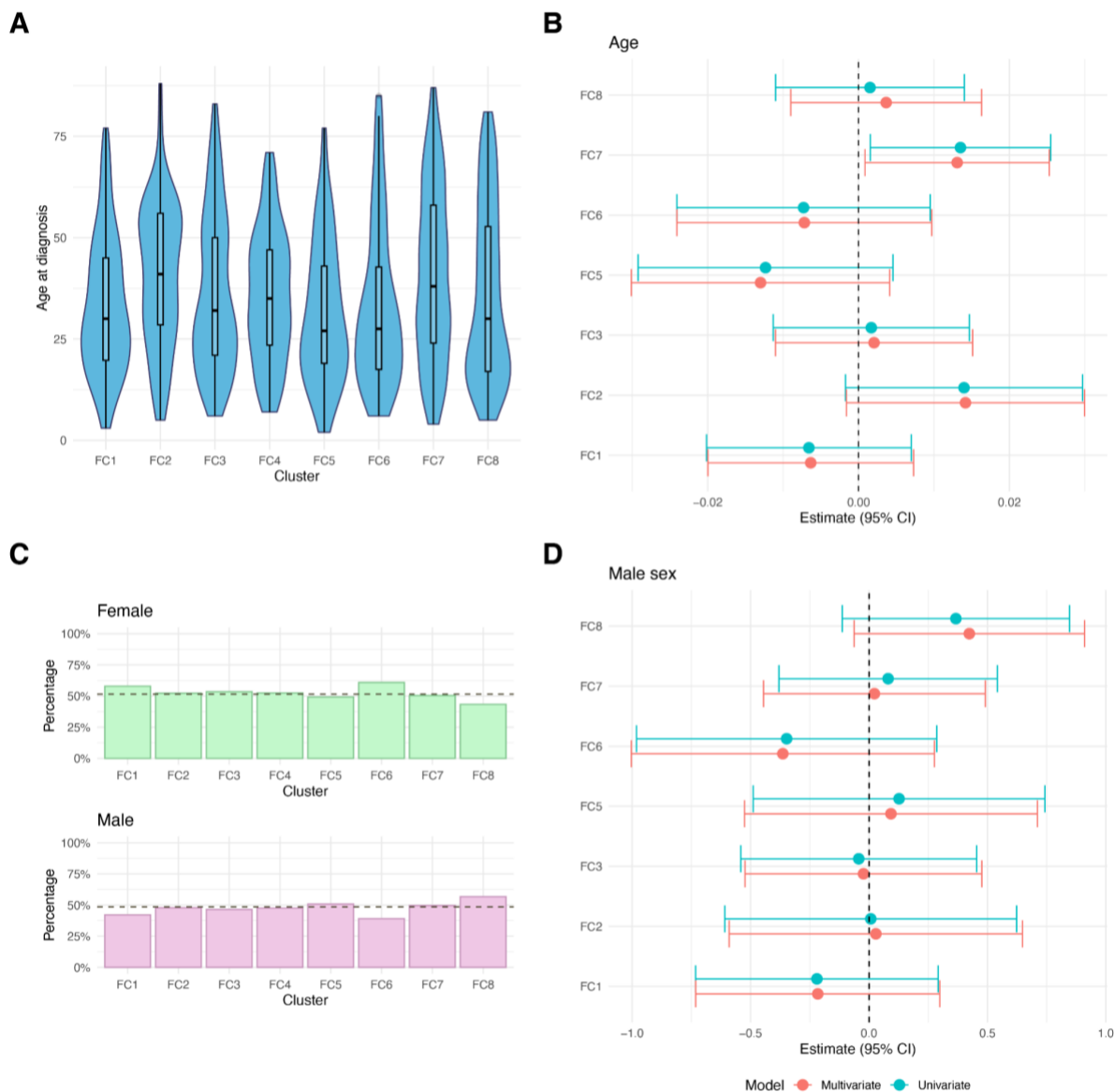
676

677

678

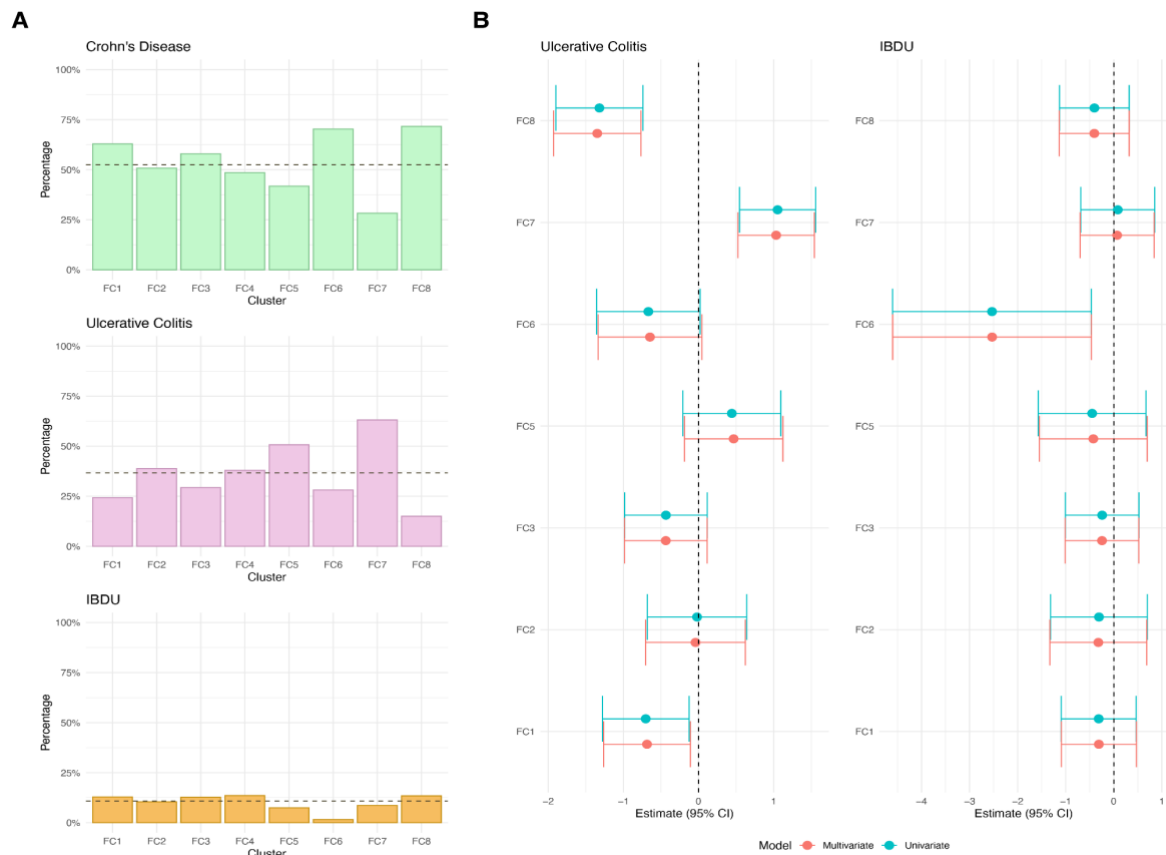
679

Figure S7. Alluvial plot demonstrating how cluster assignment changes as the number of assumed clusters increases for the chosen models for (A) faecal calprotectin and (B) C-reactive protein. The clusters found by the 8-cluster models are labelled.



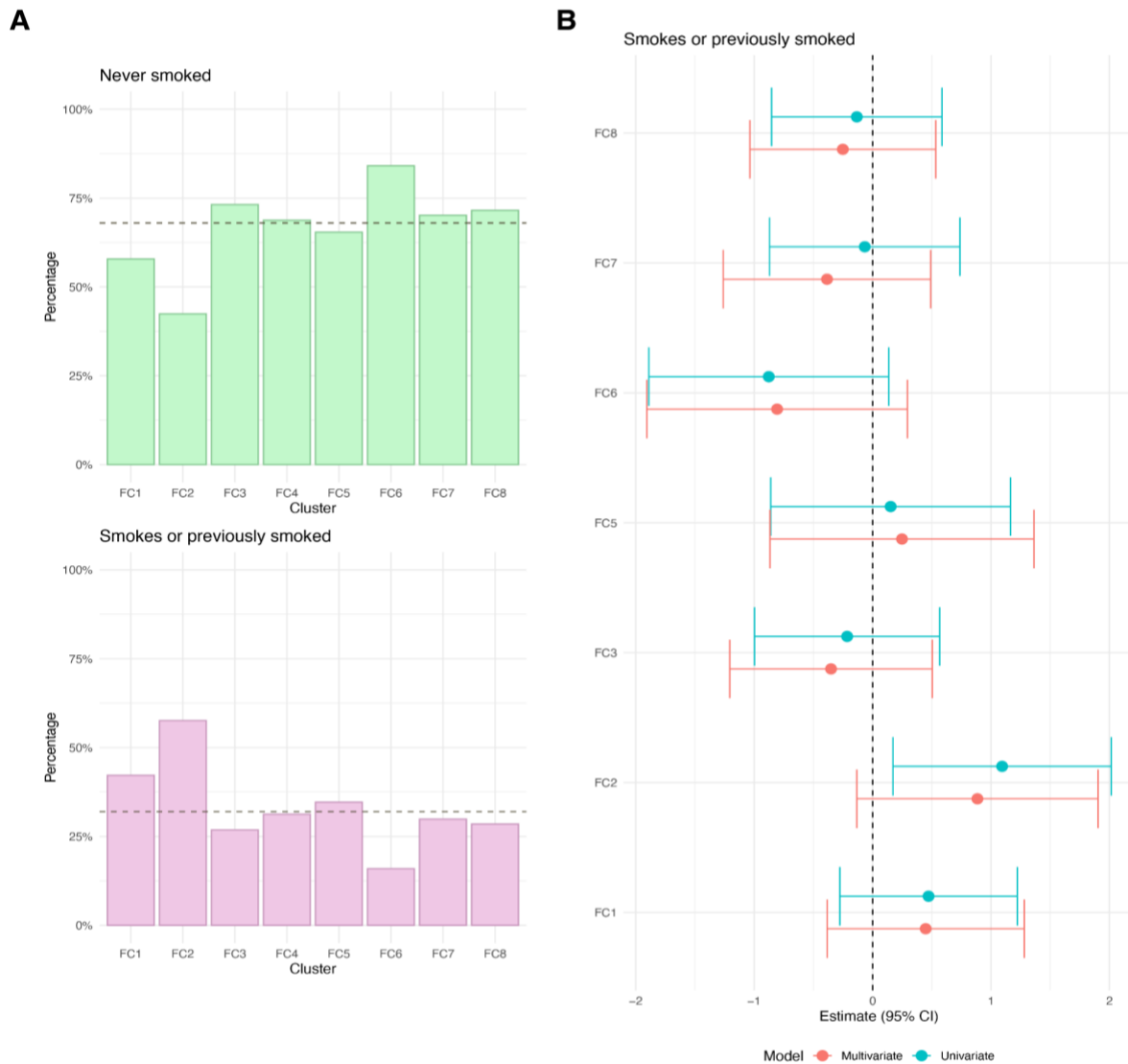
680
681
682
683
684
685
686
687
688
689
690
691

Figure S8. (A) For each FC cluster, violin plots show the distribution of age at diagnosis across subjects, highlighting median and interquartile ranges. (B) Forest plot showing the estimated effect sizes and associated 95% confidence intervals for age in a multinomial logistic regression model that uses FC cluster assignment as outcome. (C) For each FC cluster, panels show the proportion of individuals with female and male sex. The dashed horizontal line represents overall proportions across the entire FC cohort. (D) Forest plot showing the estimated effect sizes and associated 95% confidence intervals for male sex versus females (baseline category) in a multinomial logistic regression model that uses FC cluster assignment as outcome. In (B) and (C), effect sizes are with respect to the reference cluster (in this case FC4). In both cases, the multivariate model includes age, sex and IBD type as covariates. The dashed vertical lines are used as a reference to indicate no effect.



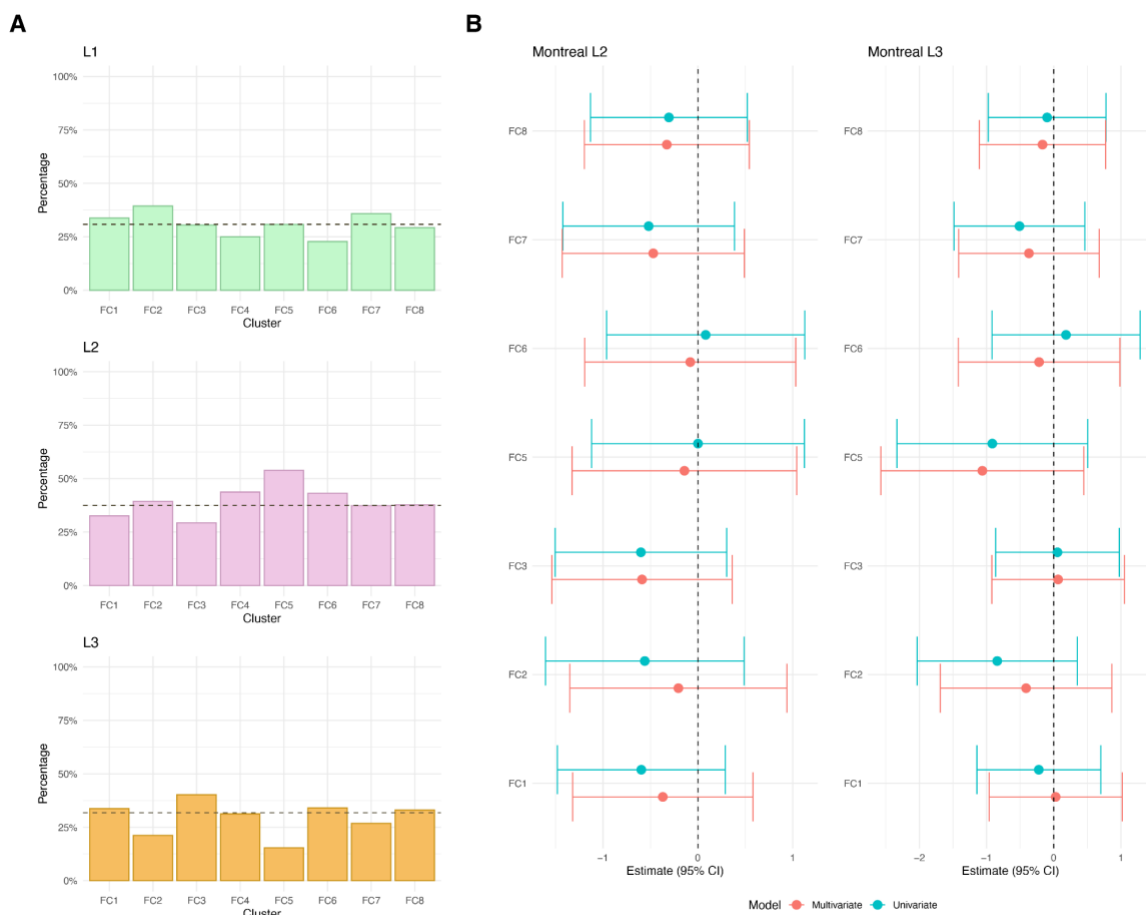
692
693
694
695
696
697
698
699
700

Figure S9. (A) For each FC cluster, panels show the proportion of individuals with Crohn's disease, ulcerative colitis and IBDU respectively. The dashed horizontal line represents overall proportions across the entire FC cohort. (B) Forest plot showing the estimated effect sizes and associated 95% confidence intervals for IBD type: ulcerative colitis and IBDU versus Crohn's disease (baseline category) in a multinomial logistic regression model that uses FC cluster assignment as outcome. Effect sizes are with respect to the reference cluster (in this case FC4). In both cases, the multivariate model includes age, sex and IBD type as covariates. The dashed vertical lines are used as a reference to indicate no effect.



701
702
703
704
705
706
707
708
709
710
711
712

Figure S10. Crohn's disease patients only. (A) For each FC cluster, panels show the proportion of individuals with smoking behaviour recorded as "no" (no and never) and "yes" (current or previously smoked) at diagnosis respectively. The dashed horizontal line represents overall proportions across the entire FC cohort. (B) Forest plot showing the estimated effect sizes and associated 95% confidence intervals for smoking: yes versus no (baseline category) in a multinomial logistic regression model that uses FC cluster assignment as outcome. Effect sizes are with respect to the reference cluster (in this case FC4). The multivariate model includes age, sex, smoking, Montreal location (L1, L2, L3), upper gastrointestinal inflammation (L4), perianal disease (yes, no) and Montreal behaviour (B1, B2/B3) as covariates. The dashed vertical lines are used as a reference to indicate no effect.



713

714

715

716

717

718

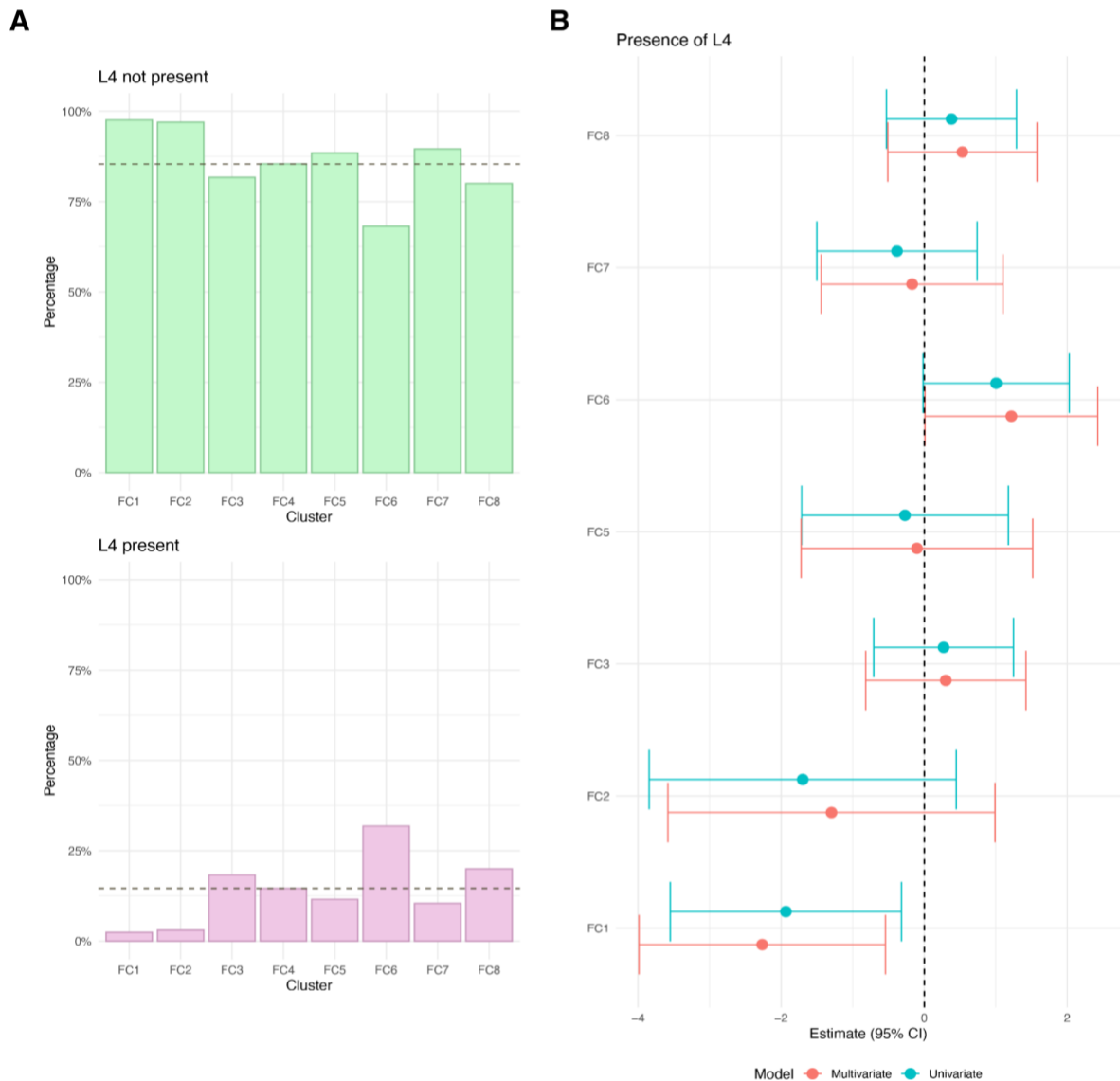
719

720

721

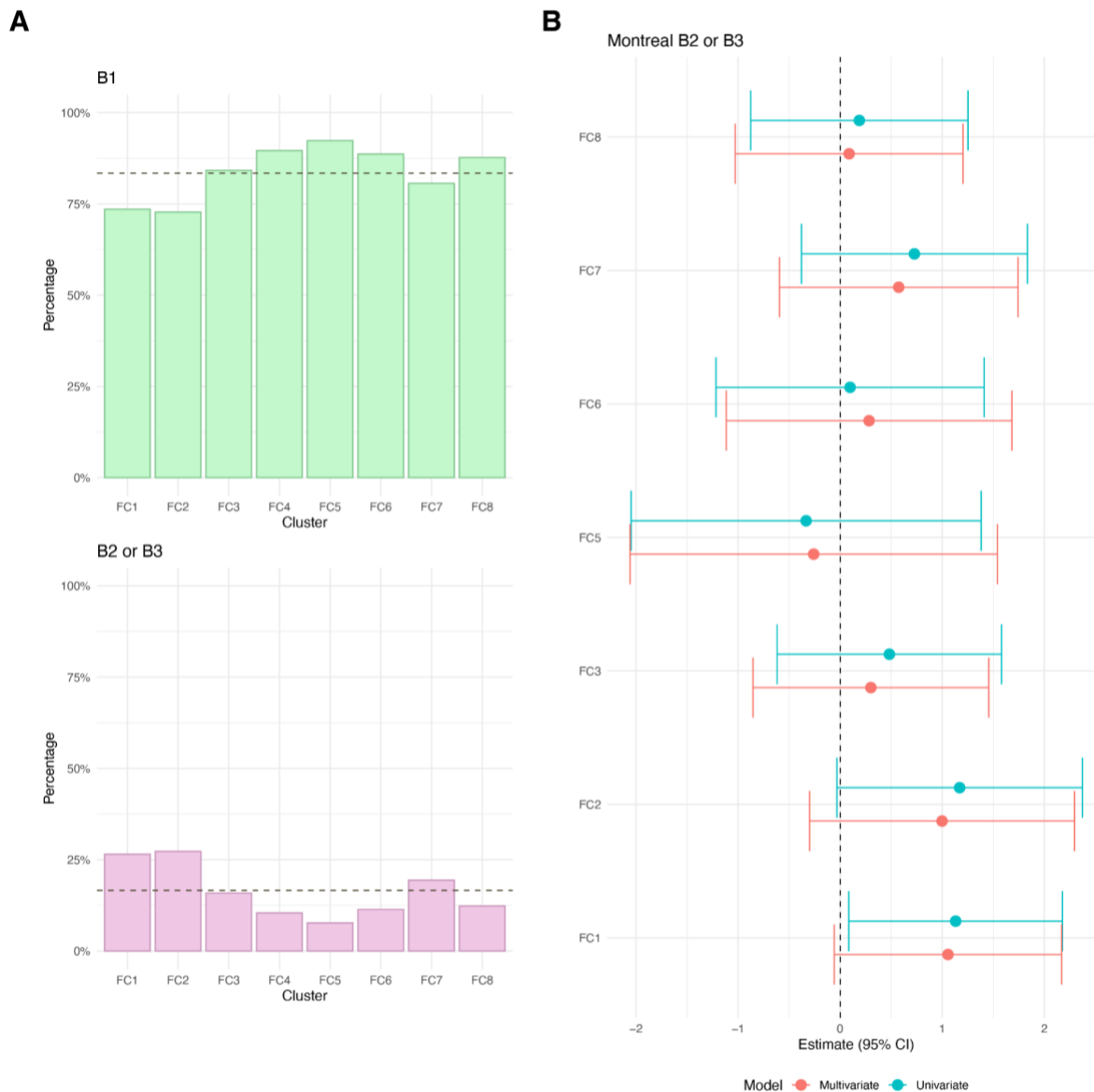
722

Figure S11. Crohn's disease patients only. (A) For each FC cluster, panels show the proportion of individuals with Montreal Location recorded as L1, L2 and L3 respectively. The dashed horizontal line represents overall proportions across the entire FC cohort. (B) Forest plot showing the estimated effect sizes and associated 95% confidence intervals for Montreal Location: L2 and L3 versus L1 (baseline category) in a multinomial logistic regression model that uses FC cluster assignment as outcome. Effect sizes are with respect to the reference cluster (in this case FC4). The multivariate model includes age, sex, smoking, Montreal location (L1, L2, L3), upper gastrointestinal inflammation (L4), perianal disease (yes, no) and Montreal behaviour (B1, B2/B3) as covariates. The dashed vertical lines are used as a reference to indicate no effect.



723
724
725
726
727
728
729
730
731
732

Figure S12 Crohn's disease patients only. (A) For each FC cluster, panels show the proportion of individuals with Montreal L4 (upper gastrointestinal inflammation), recorded as present or non present. The dashed horizontal line represents overall proportions across the entire FC cohort. (B) Forest plot showing the estimated effect sizes and associated 95% confidence intervals for L4: present versus not present (baseline category) in a multinomial logistic regression model that uses FC cluster assignment as outcome. Effect sizes are with respect to the reference cluster (in this case FC4). The multivariate model includes age, sex, smoking, Montreal location (L1, L2, L3), upper gastrointestinal inflammation (L4), perianal disease (yes, no) and Montreal behaviour (B1, B2/B3) as covariates. The dashed vertical lines are used as a reference to indicate no effect.



733

734

735 *Figure S13. Crohn's disease patients only. (A) For each FC cluster, panels show the proportion of*
 736 *individuals with Montreal behaviour recorded as B1 or B2/B3 respectively. The dashed horizontal line*

737

738 *represents overall proportions across the entire FC cohort. (B) Forest plot showing the estimated*
 739 *effect sizes and associated 95% confidence intervals for Montreal behaviour: B2/B3 versus B1*

740

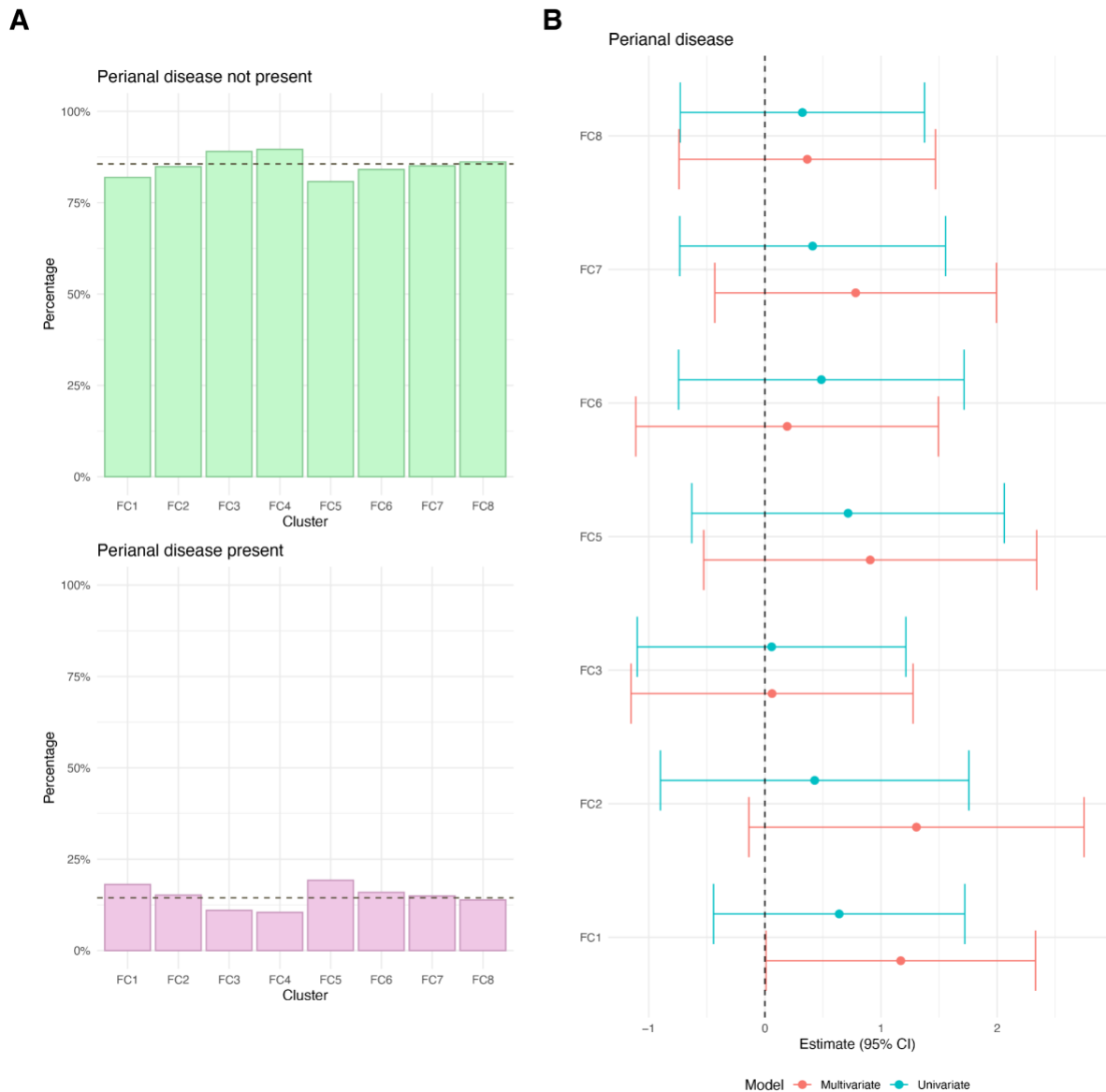
741 *(baseline category) in a multinomial logistic regression model that uses FC cluster assignment as*
 742 *outcome. Effect sizes are with respect to the reference cluster (in this case FC4). The multivariate*

743

744 *model includes age, sex, smoking, Montreal location (L1, L2, L3), upper gastrointestinal inflammation*
 745 *(L4), perianal disease (yes, no) and Montreal behaviour (B1, B2/B3) as covariates. The dashed*

746

747 *vertical lines are used as a reference to indicate no effect.*



743

744

745

746

747

748

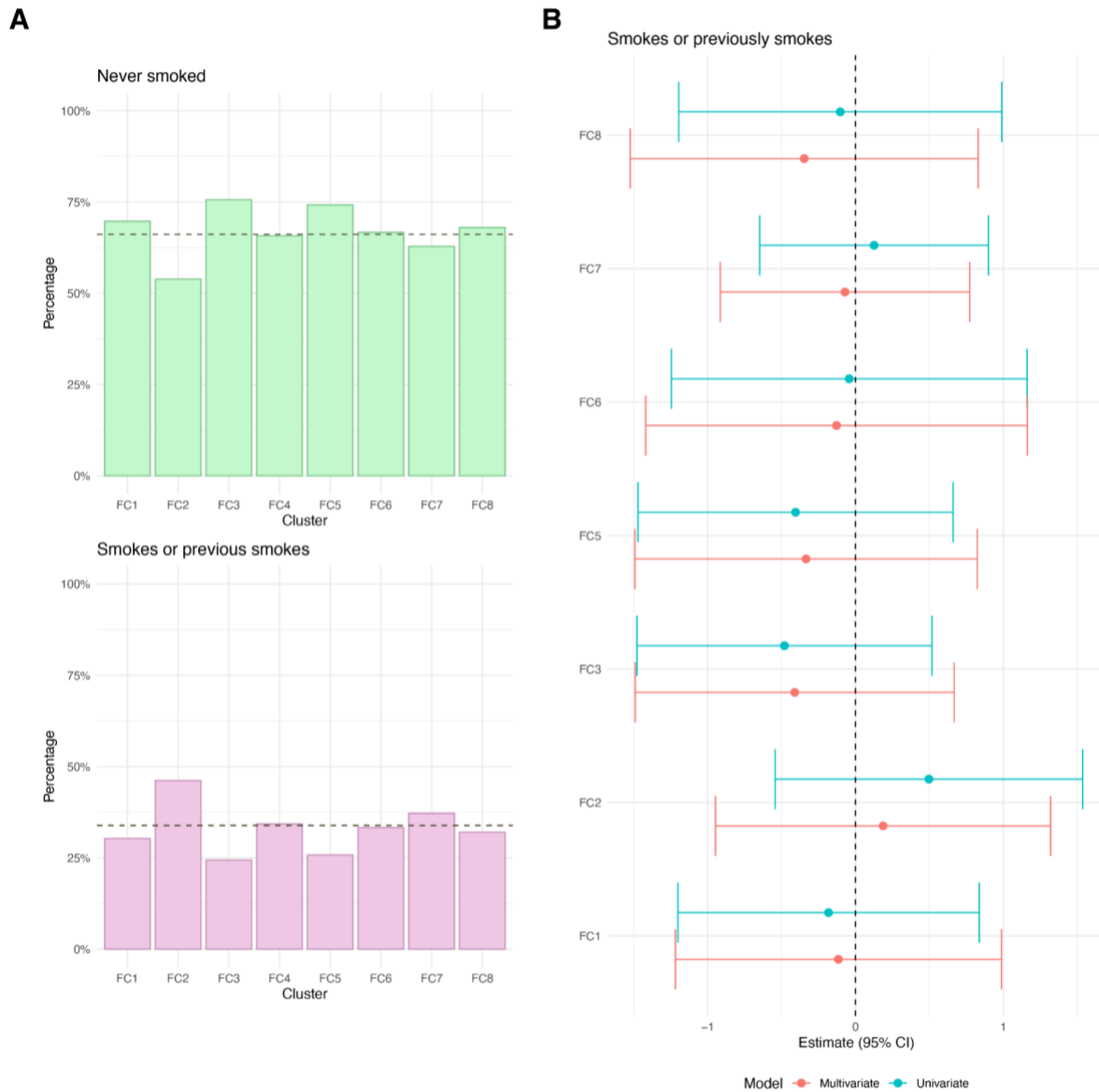
749

750

751

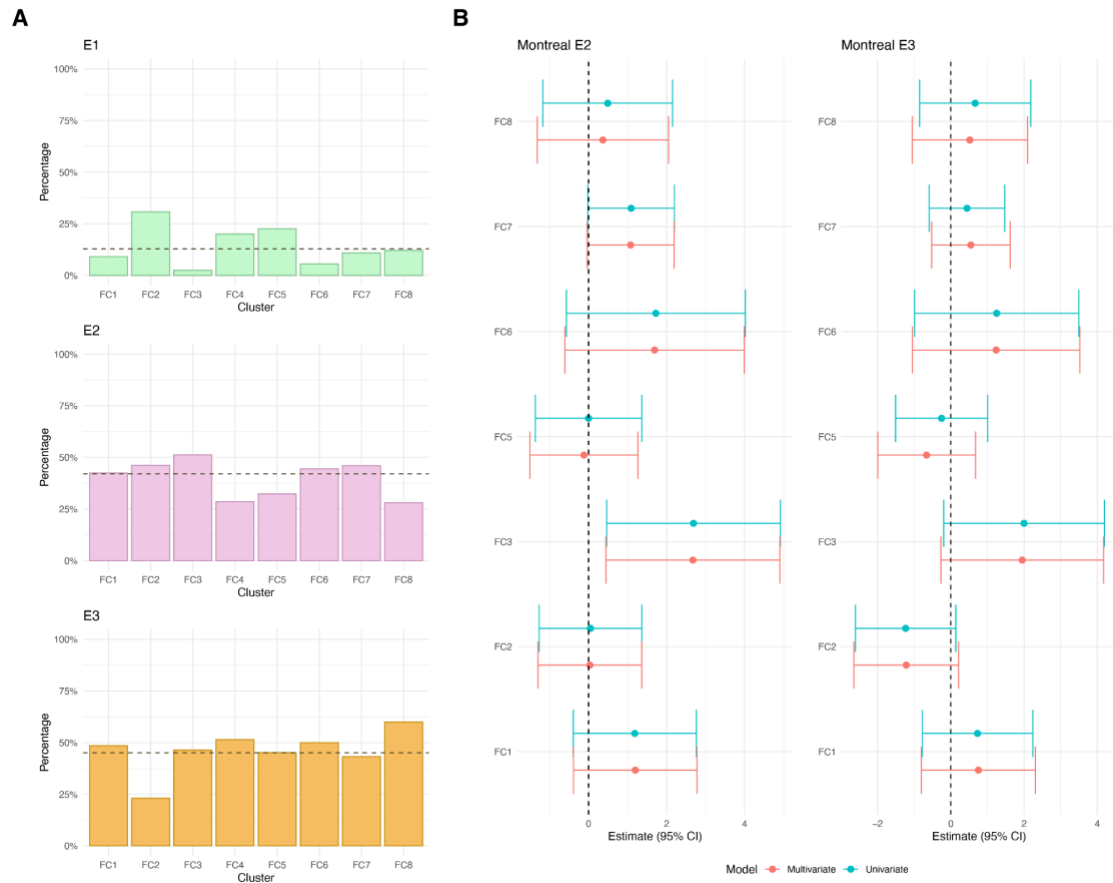
752

Figure S14 Crohn's disease patients only. (A) For each FC cluster, panels show the proportion of individuals with perianal disease recorded as present or not present. The dashed horizontal line represents overall proportions across the entire FC cohort. (B) Forest plot showing the estimated effect sizes and associated 95% confidence intervals for perianal disease: present versus not present (baseline category) in a multinomial logistic regression model that uses FC cluster assignment as outcome. Effect sizes are with respect to the reference cluster (in this case FC4). The multivariate model includes age, sex, smoking, Montreal location (L1, L2, L3), upper gastrointestinal inflammation (L4), perianal disease (yes, no) and Montreal behaviour (B1, B2/B3) as covariates. The dashed vertical lines are used as a reference to indicate no effect.



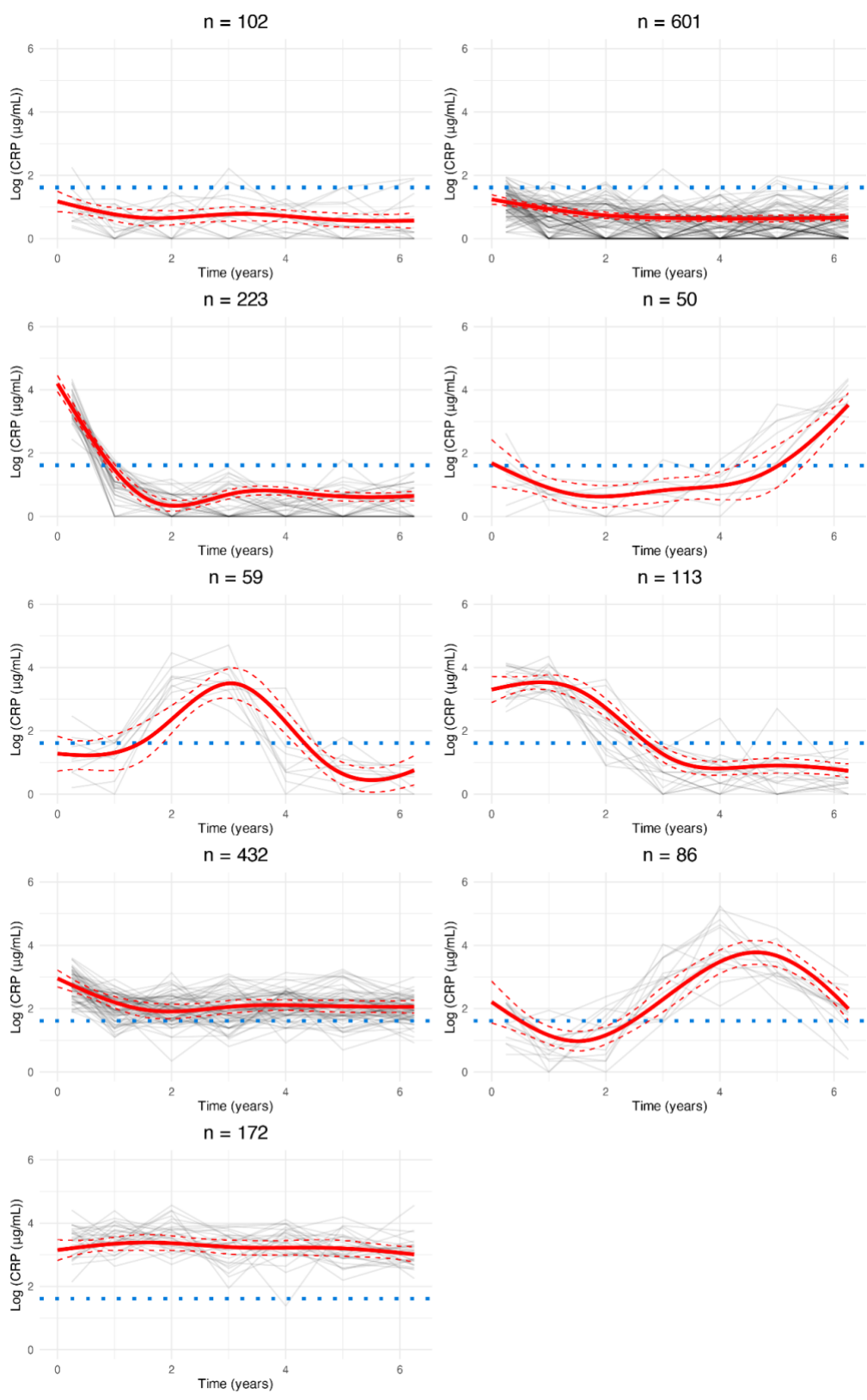
753
754
755
756
757
758
759
760
761
762

Figure S15. Ulcerative colitis patients only. (A) For each FC cluster, panels show the proportion of individuals with smoking behaviour recorded as “no” (no and never) and “yes” (current or previously smoked) at diagnosis respectively. The dashed horizontal line represents overall proportions across the entire FC cohort. (B) Forest plot showing the estimated effect sizes and associated 95% confidence intervals for smoking: yes versus no (baseline category) in a multinomial logistic regression model that uses FC cluster assignment as outcome. Effect sizes are with respect to the reference cluster (in this case FC4). The multivariate model includes age, sex, smoking and Montreal extent (E1, E2, E3). The dashed vertical lines are used as a reference to indicate no effect.



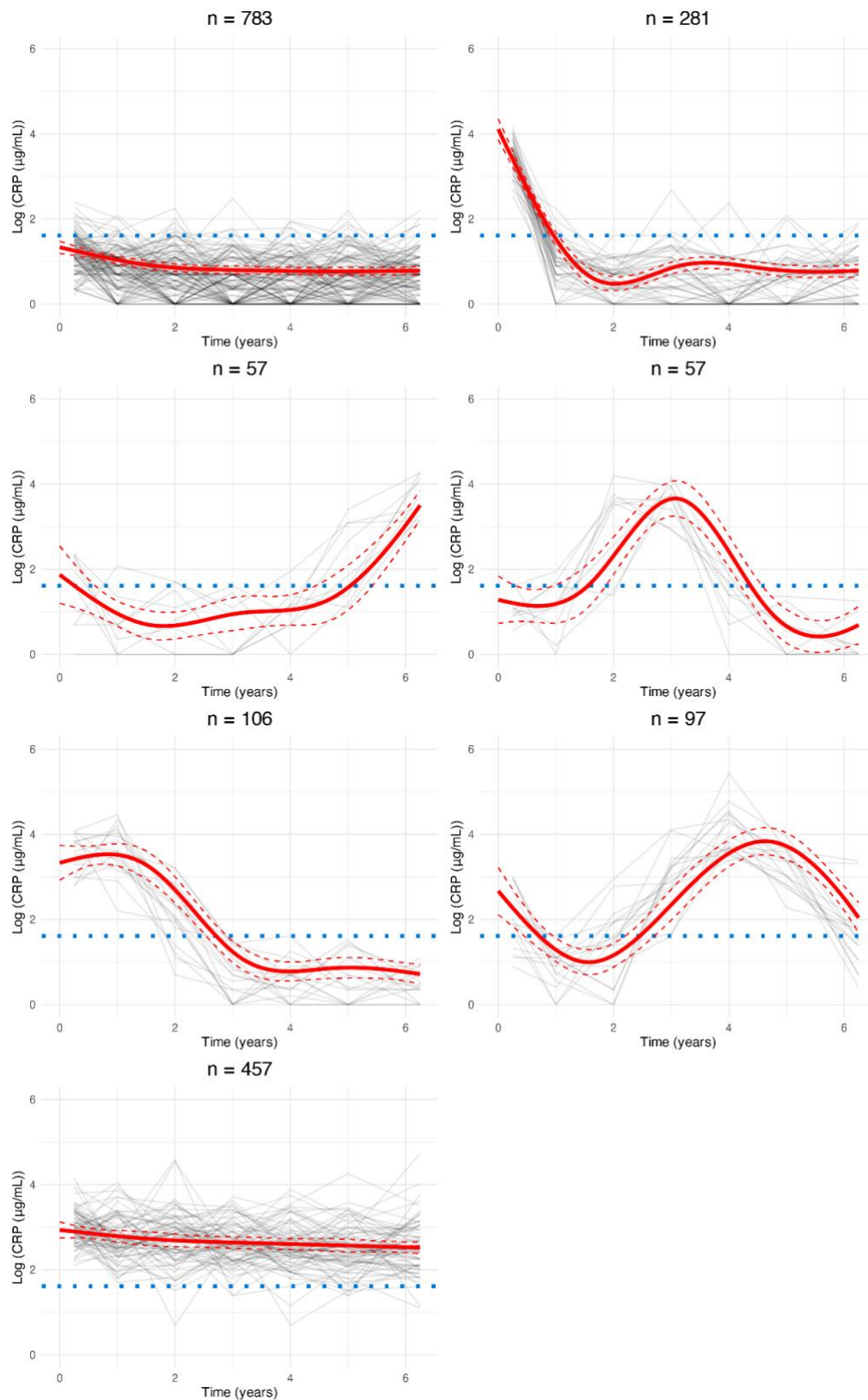
763
764
765
766
767
768
769
770
771

Figure S16. Ulcerative colitis patients only. (A) For each cluster, panels show the proportion of individuals with Montreal extent recorded as E1, E2 and E3 respectively. The dashed horizontal line represents overall proportions across the entire FC cohort. (B) Forest plot showing the estimated effect sizes and associated 95% confidence intervals for Montreal extent: E2 and E3 versus E1 (baseline category) in a multinomial logistic regression model that uses FC cluster assignment as outcome. Effect sizes are with respect to the reference cluster (in this case FC4). The multivariate model includes age, sex, smoking and Montreal extent (E1, E2, E3). The dashed vertical lines are used as a reference to indicate no effect.



772
773
774
775
776

Figure S17. Cluster trajectories obtained from LCMM assuming nine clusters fitted to C-reactive protein data. Red lines indicate predicted mean cluster profiles with 95% confidence intervals. Dotted horizontal lines indicate log(5µg/mL). For visualisation purposes, pseudo subject-specific trajectories have been generated by amalgamating observations from groups of six subjects.



777

778

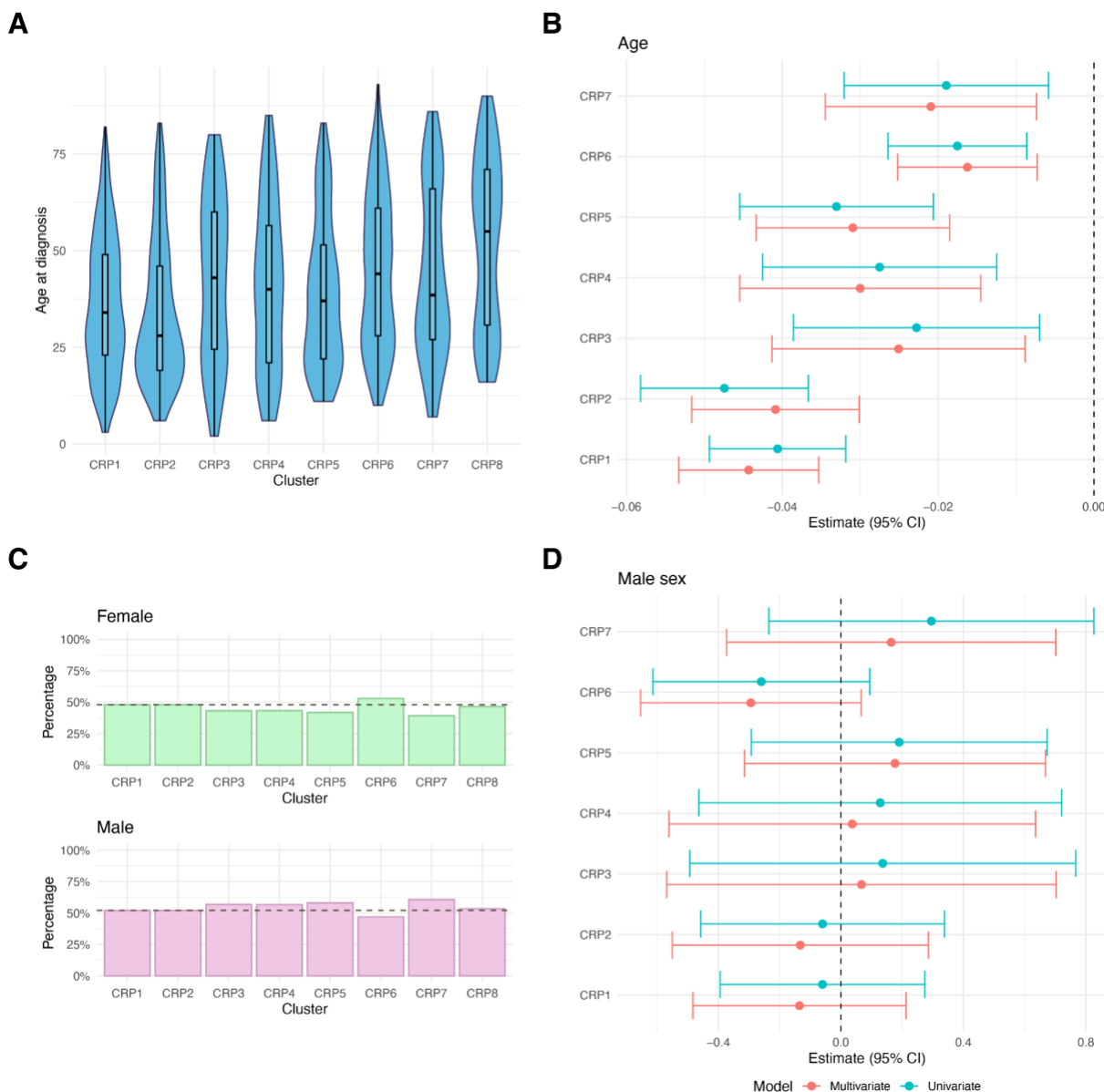
779

780

781

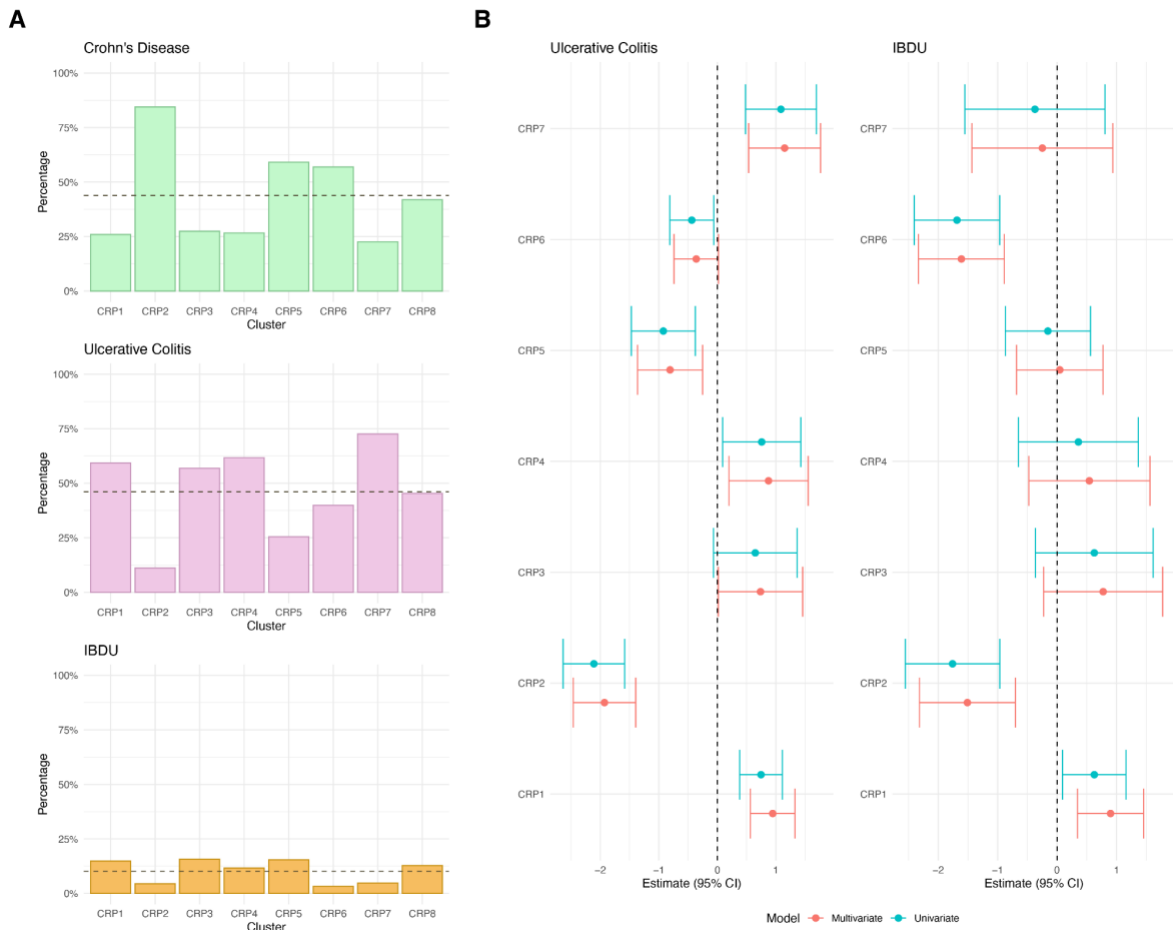
782

Figure S18. Cluster trajectories obtained from LCMC assuming seven clusters fitted to C-reactive protein data. Red lines indicate predicted mean cluster profiles with 95% confidence intervals. Dotted horizontal lines indicate log(5 μg/mL). For visualisation purposes, pseudo subject-specific trajectories have been generated by amalgamating observations from groups of six subjects.



783
784
785
786
787
788
789
790
791
792
793
794

Figure S19. (A) For each CRP cluster, violin plots show the distribution of age at diagnosis across subjects, highlighting median and interquartile ranges. (B) Forest plot showing the estimated effect sizes and associated 95% confidence intervals for age in a multinomial logistic regression model that uses CRP cluster assignment as outcome. (C) For each CRP cluster, panels show the proportion of individuals with female and male sex. The dashed horizontal line represents overall proportions across the entire CRP cohort. (D) Forest plot showing the estimated effect sizes and associated 95% confidence intervals for male sex versus females (baseline category) in a multinomial logistic regression model that uses CRP cluster assignment as outcome. In (B) and (C), effect sizes are with respect to the reference cluster (in this case CRP8). In both cases, the multivariate model includes age, sex and IBD type as covariates. The dashed vertical lines are used as a reference to indicate no effect.



795

796 *Figure S20. (A) For each CRP cluster, panels show the proportion of individuals with Crohn's disease,*

797 *ulcerative colitis and IBDU respectively. The dashed horizontal line represents overall proportions*

798 *across the entire CRP cohort. (B) Forest plot showing the estimated effect sizes and associated 95%*

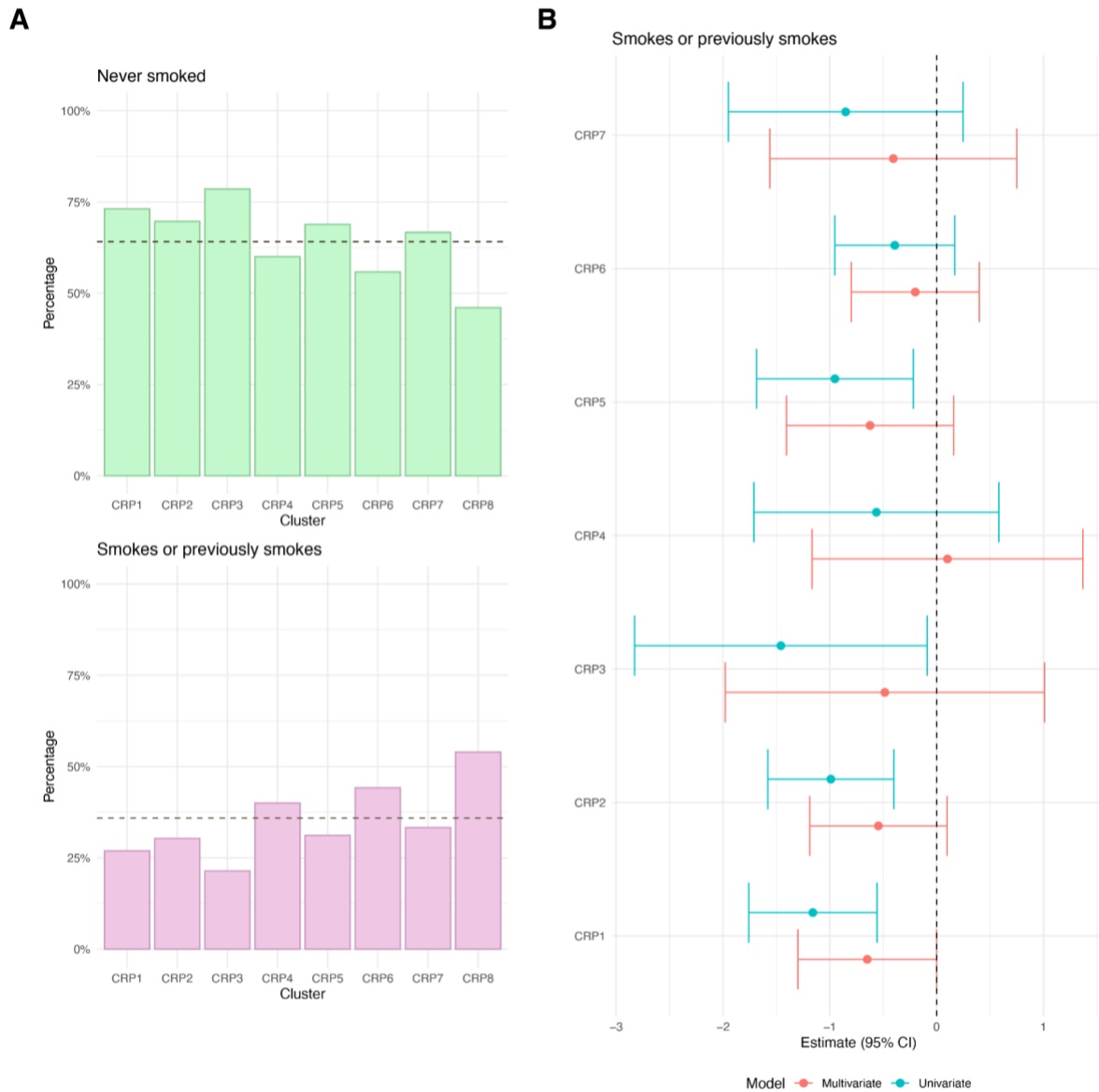
799 *confidence intervals for IBD type: ulcerative colitis and IBDU versus Crohn's disease (baseline*

800 *category) in a multinomial logistic regression model that uses CRP cluster assignment as outcome.*

801 *Effect sizes are with respect to the reference cluster (in this case CRP8). In both cases, the*

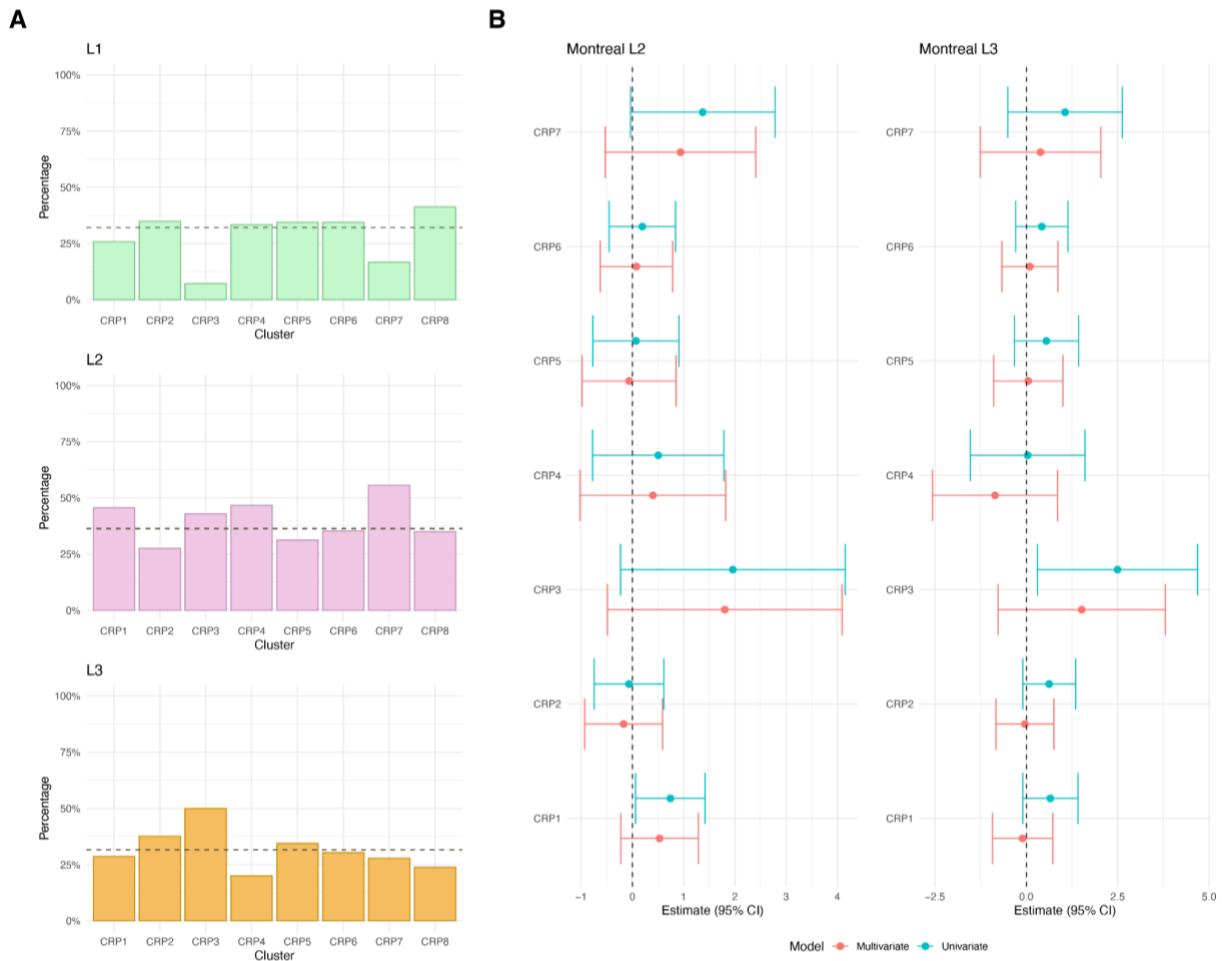
802 *multivariate model includes age, sex and IBD type as covariates. The dashed vertical lines are used*

803 *as a reference to indicate no effect.*



804
805
806
807
808
809
810
811
812
813

Figure S21. Crohn's disease patients only. (A) For each CRP cluster, panels show the proportion of individuals with smoking behaviour recorded as "no" (no and never) and "yes" (current or previously smoked) at diagnosis respectively. The dashed horizontal line represents overall proportions across the entire CRP cohort. (B) Forest plot showing the estimated effect sizes and associated 95% confidence intervals for smoking: yes versus no (baseline category) in a multinomial logistic regression model that uses CRP cluster assignment as outcome. Effect sizes are with respect to the reference cluster (in this case CRP8). The multivariate model includes age, sex, smoking, Montreal location (L1, L2, L3), upper gastrointestinal inflammation (L4), and Montreal behaviour (B1, B2/B3) as covariates. The dashed vertical lines are used as a reference to indicate no effect.



814

815

816

817

818

819

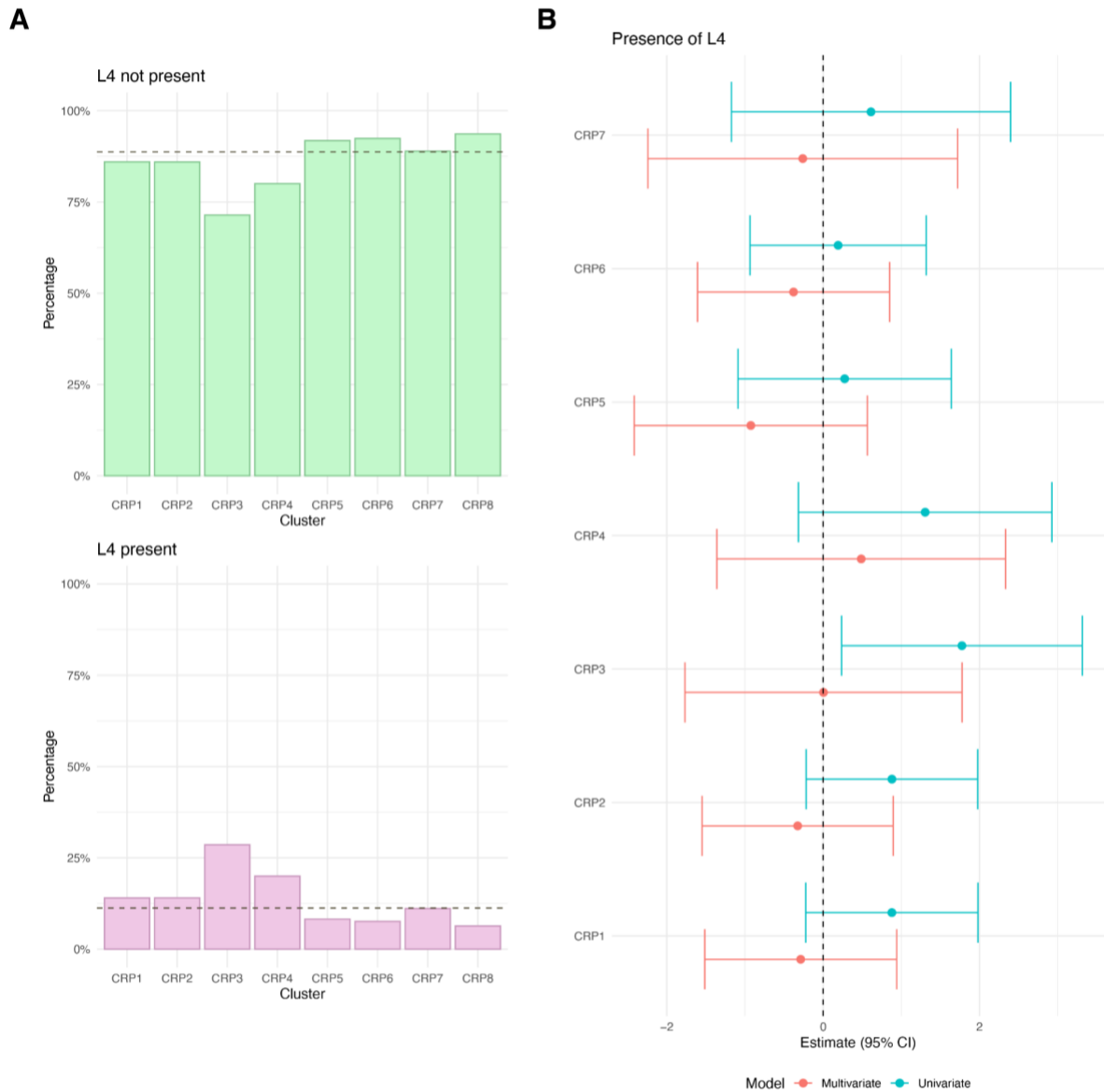
820

821

822

823

Figure S22. Crohn's disease patients only. (A) For each CRP cluster, panels show the proportion of individuals with Montreal Location recorded as L1, L2 and L3 respectively. The dashed horizontal line represents overall proportions across the entire CRP cohort. (B) Forest plot showing the estimated effect sizes and associated 95% confidence intervals for Montreal Location: L2 and L3 versus L1 (baseline category) in a multinomial logistic regression model that uses CRP cluster assignment as outcome. Effect sizes are with respect to the reference cluster (in this case CRP8). The multivariate model includes age, sex, smoking, Montreal location (L1, L2, L3), upper gastrointestinal inflammation (L4), and Montreal behaviour (B1, B2/B3) as covariates. The dashed vertical lines are used as a reference to indicate no effect.



824

825

826

827

828

829

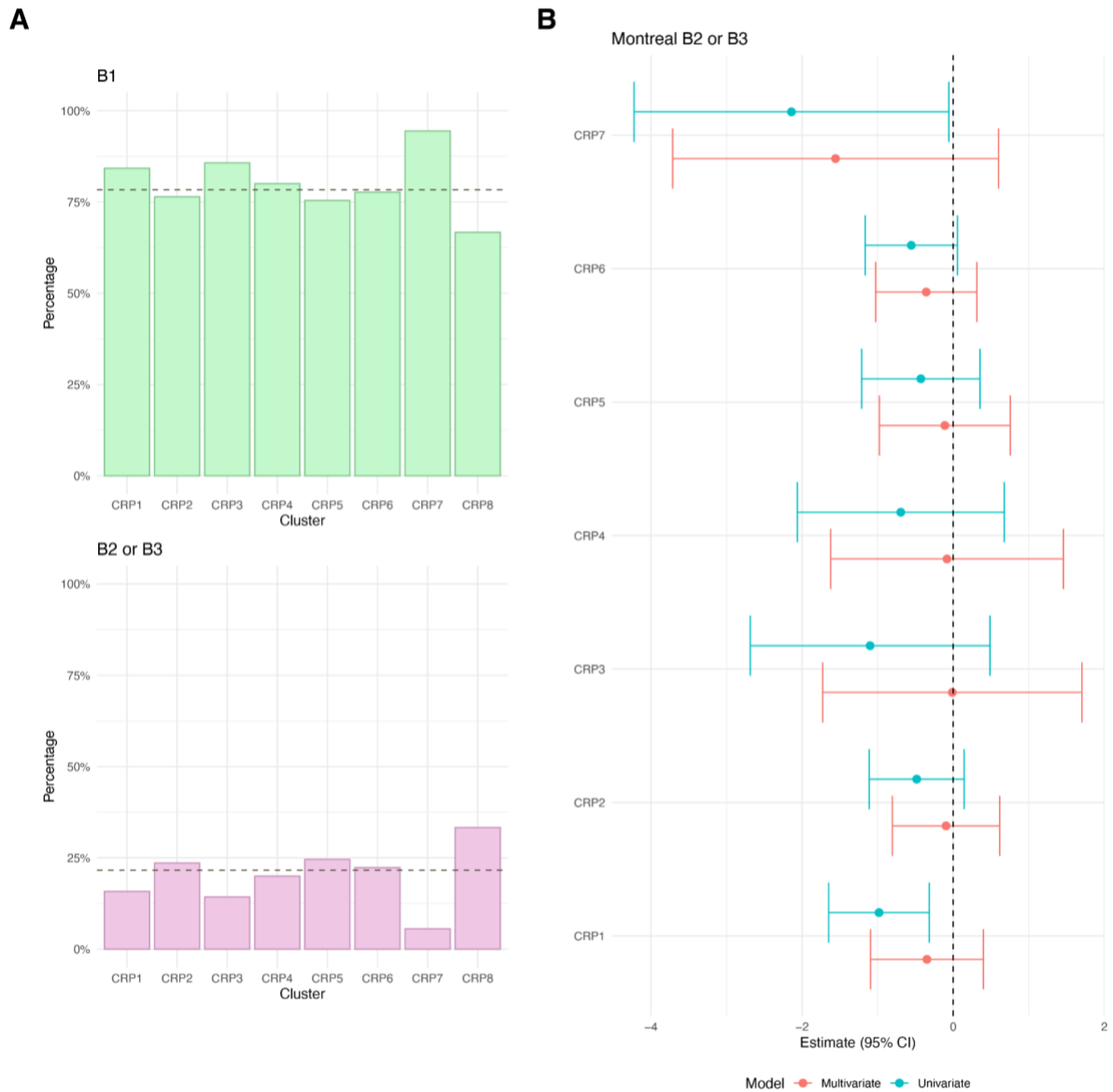
830

831

832

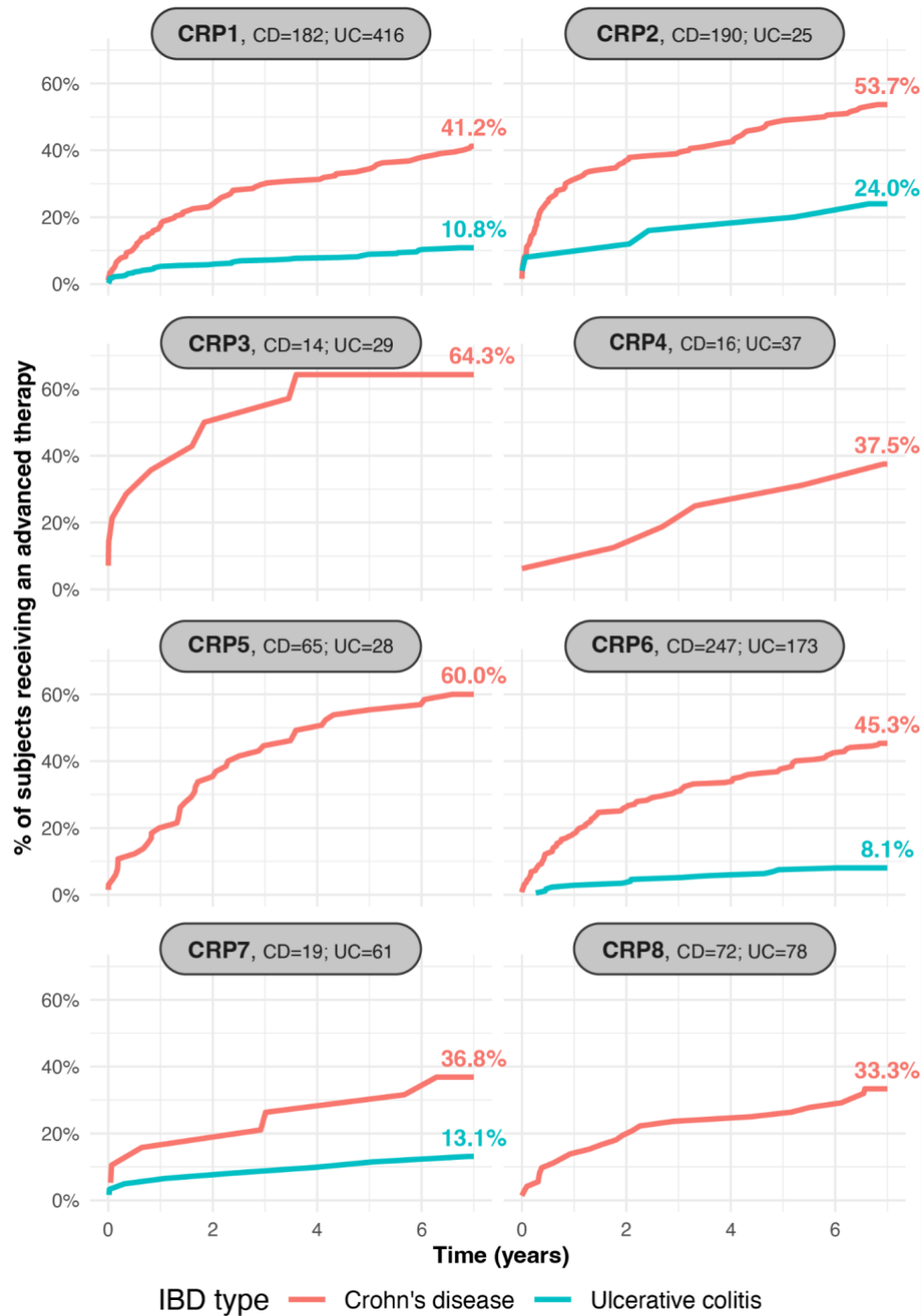
833

Figure S23. Crohn's disease patients only. (A) For each CRP cluster, panels show the proportion of individuals with Montreal L4 (upper gastrointestinal inflammation), recorded as present or non present. The dashed horizontal line represents overall proportions across the entire CRP cohort. (B) Forest plot showing the estimated effect sizes and associated 95% confidence intervals for L4: present versus not present (baseline category) in a multinomial logistic regression model that uses CRP cluster assignment as outcome. Effect sizes are with respect to the reference cluster (in this case CRP8). The multivariate model includes age, sex, smoking, Montreal location (L1, L2, L3), upper gastrointestinal inflammation (L4), and Montreal behaviour (B1, B2/B3) as covariates. The dashed vertical lines are used as a reference to indicate no effect.



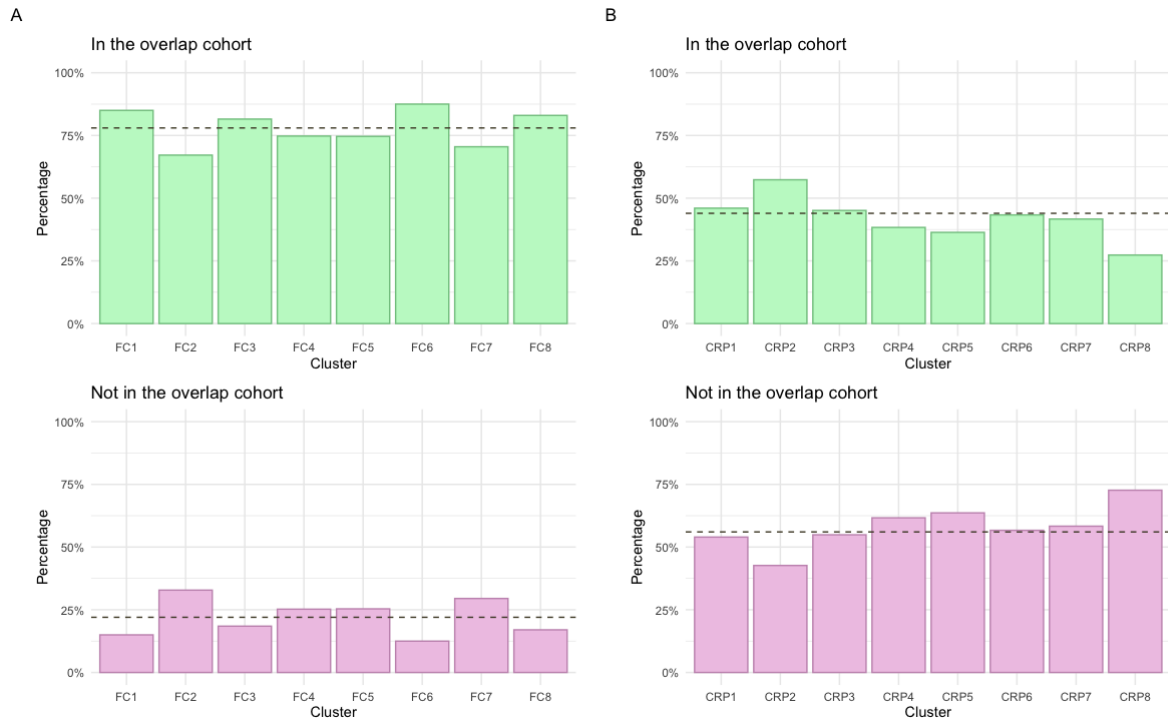
834
835
836
837
838
839
840
841
842
843

Figure S24. Crohn's disease patients only. (A) For each CRP cluster, panels show the proportion of individuals with Montreal behaviour recorded as B1 or B2/B3 respectively. The dashed horizontal line represents overall proportions across the entire CRP cohort. (B) Forest plot showing the estimated effect sizes and associated 95% confidence intervals for Montreal behaviour: B2/B3 versus B1 (baseline category) in a multinomial logistic regression model that uses CRP cluster assignment as outcome. Effect sizes are with respect to the reference cluster (in this case CRP8). The multivariate model includes age, sex, smoking, Montreal location (L1, L2, L3), upper gastrointestinal inflammation (L4), and Montreal behaviour (B1, B2/B3) as covariates. The dashed vertical lines are used as a reference to indicate no effect.



844
845
846
847
848
849

Figure S25. CRP cluster-specific cumulative distribution for first-line advanced therapy prescribing for Crohn's disease (red) and ulcerative colitis (teal) subjects. Clusters are ordered from lowest (CRP1) to highest (CRP8) cumulative inflammatory burden. The number of CD and UC subjects present in each cluster is displayed as panel titles. Curves which would describe fewer than five subjects are not shown.



850
851
852
853
854
855

Figure S26. (A) For each FC cluster, panels show the proportion of individuals included in the overlap cohort, which consists of subjects included in both the FC and CRP analysis. The dashed horizontal line represents overall proportions across the entire FC cohort. (B) As in (A), but focusing on CRP clusters instead. The dashed horizontal line represents overall proportions across the entire CRP cohort.

856 Supplemental tables

Clusters	Maximum log-likelihood	AIC	BIC
2	-16532.10	33094.20	33168.35
3	-16354.39	32754.78	32868.47
4	-16260.21	32582.42	32735.66
5	-16201.86	32481.71	32674.49
6	-16141.82	32377.63	32609.96
7	-16109.77	32329.54	32601.42
8	-16076.89	32279.77	32591.19
9	-16039.66	32221.33	32572.29
10	-16015.29	32188.59	32579.09

857 *Table S1. Likelihood-based model statistics for LCMMs fitted to faecal calprotectin data across 2–10*
 858 *clusters using the chosen model specification. Boldface font indicates optimal values.*

Clusters	Maximum log-likelihood	AIC	BIC
2	-15451.41	30932.82	31015.57
3	-15314.76	30675.52	30802.40
4	-15240.15	30542.29	30713.30
5	-15173.04	30424.09	30639.23
6	-15106.25	30306.50	30565.78
7	-15051.43	30212.86	30516.27
8	-15016.96	30159.91	30507.45
9	-15014.76	30171.53	30563.20
10	-15014.40	30186.81	30622.61

859 *Table S2. Likelihood-based model statistics for LCMMs fitted to processed CRP data across 2–10*
 860 *clusters using the chosen model specification. Boldface font indicates optimal values.*

861